LA-UR-15-29376
Approved for public release; distribution is unlimited.

Title: Assessment of Residual Stresses in 3013 Inner and Outer Containers and Teardrop Samples

Author(s): Stroud, Mary Ann
Prime, Michael Bruce
Veirs, Douglas Kirk
Berg, John M.
Clausen, Bjorn
Worl, Laura Ann
DeWald, Adrian

Intended for: Report

Issued: 2015-12-08

Assessment of Residual Stresses in 3013 Inner and Outer Containers and Teardrop Samples

M.A. Stroud*, M.B. Prime*, D.K. Veirs*, J.M. Berg*, B. Clausen*, Laura A. Worl*, and A.T. DeWald#

* Los Alamos National Laboratory, # Hill Engineering, LLC

I. INTRODUCTION

The Department of Energy's (DOE's) 3013 Standard for packaging plutonium-bearing materials for storage up to fifty years specifies a minimum of two individually welded, nested containers, herein referred to as the 3013 outer and the 3013 inner. Figure 1 shows an intact outer container and cutaways of the three components of a typical configuration, in this case the British Nuclear Fuels, Ltd. (BNFL)-designed outer, inner, and convenience containers used at Rocky Flats Environmental Technology Site (RFETS). Convenience containers are required to not be sealed and do not perform the same function as the inner and outer containers.

Figure 1. BNFL designed outer, inner, and convenience containers.

Stress corrosion cracking (SCC) has been identified as a potential failure mechanism for 3013 inner containers which could result in the integrity of the Safety Class outer container being considered indeterminate.[1] SCC susceptibility studies indicated that 3013 outer containers, which are the same design for all sites in the DOE complex that package 3013 containers, and Savannah River Site (SRS)/Hanford inner containers contain sufficient residual stress to crack under extreme conditions (boiling $MgCl_2$). RFETS and Lawrence Livermore National Laboratory (LLNL) inner containers are less likely than SRS and Hanford containers to exhibit SCC and have not been tested using boiling $MgCl_2$.[2] Stress corrosion cracking is induced from the combined influences of tensile stress, a corrosive environment and a susceptible material. This report discusses residual stresses in the 3013 outer, the SRS/Hanford and RFETS/LLNL inner containers, and teardrop samples used in studies to assess the potential for SCC in 3013 containers. Residual tensile stresses in the heat affected zones of the closure welds are of particular concern.[2]

Table 1 shows pictures, identifies the material of construction, shows cross section of the weld of interest, and identifies the welding techniques used for a 3013 outer container, a SRS/Hanford inner container, a RFETS/LLNL inner container, and a teardrop sample.

Table 1. Pictures, material of construction, weld cross section, and welding technique for the items studied.

Sample Type	Sample Picture	Material of Construction Stainless Steel (SS)	Sample Weld Region	Welding Technique
3013 outer container		316L		Gas Tungsten Arc Weld (GTAW) or Laser
SRS/Hanford 3013 Inner Container		304L	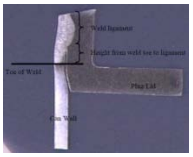	GTAW
RFETS/LLNL 3013 inner container		ASTM A240 316		Laser
Teardrop sample	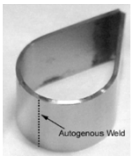	304L	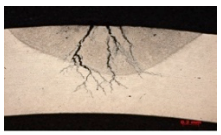	GTAW

Additional information on container materials and fabrication may be found in Dunn et al.[3] Several authors have measured a threshold stress for SCC in 300 series austenitic stainless steel.[4] Results varied with corrosive conditions and test duration but results on the order of 100 MPa were common. Results as low as ~15MPa were reported under the severe condition of boiling $MgCl_2$.[4]

II. 3013 OUTER CONTAINER STUDIES

3013 Outer Container

The 3013 outer container that was studied consisted of a BNFL outer container body made from 316L SS seamless pipe, a 316L SS plate as a base and a 316L SS plate as a lid. A smooth and continuous full penetration autogenous weld ~0.5" from bottom of container was used to connect the container body to the base plate. The lid was press fit into the body with a possible interference up to 0.07 mm. Prior to creating the closure weld, seven small tack welds were made sequentially and placed symmetrically around the container; with the eighth position being the weld start position. The container was then sealed with a GTAW autogenous closure weld that fully consumed the tacks.[3] During welding, a 5 second preheat occurred at the weld start, then the weld was created using an average travel speed of 0.50 to 0.56 rpm during the first 135° of travel, and from 0.57 to 0.63 rpm during the remainder of the weld. Welding continued several degrees past the start position before stopping.[5] Boiling $MgCl_2$ SCC susceptibility

studies identified the base-to-container weld and the closure weld as susceptible locations for SCC in 3013 outer containers.[2]

Outer Container Experimental Methods

Neutron diffraction and the contour method were used to measure residual stresses in a 3013 outer container. Detailed information on these techniques may be found elsewhere.[6]

Neutron Diffraction Measurements

Neutron diffraction was used to determine residual stresses in the outer container closure weld region (OCCWR) and lid region of a 3013 outer container. Neutron Diffraction is used to determine the crystal lattice spacing, and the spacing is used as an intrinsic "strain gauge." Changes in the lattice spacing indicate the state of strain in the sample per the equation

$$\varepsilon = \frac{d - d_0}{d_0}$$

where ε is the elastic strain, d is the lattice spacing in the "stressed" material and d_0 is the unstressed lattice spacing. Residual stress may then be calculated from the measured strain using Hooke's Law for isotropic elasticity:

$$\sigma_i = \frac{E(1-\nu)}{(1+\nu)(1-2\nu)}\left[\varepsilon_i + \frac{\nu}{1-\nu}(\varepsilon_j + \varepsilon_k)\right], \quad i, j, k = r, \theta, z$$

Where E is Young's modulus and ν is Poisson's ratio.

The intact Hanford 3013 outer container used for the neutron diffraction measurements was H003085 with lid EPD L00002 P02779 and weld sticker: Welded 6/22/03, 2Z-03-0054, No BTC Surrogate. Figure 2 shows the closure weld of the container.

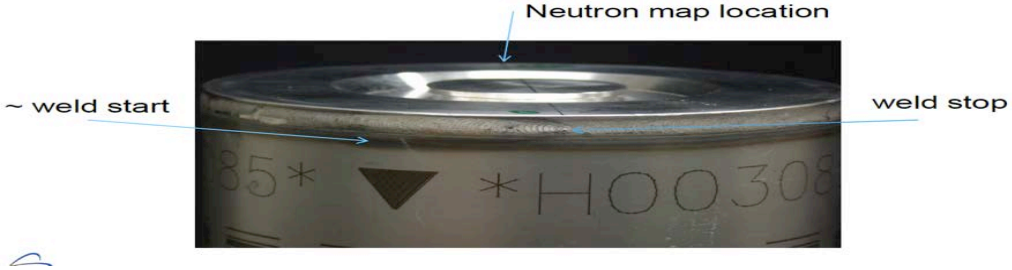

Figure 2. 3013 outer container H003085 used for neutron diffraction measurement.

A small thin specimen was cut from a second companion Hanford 3013 outer container to relieve residual stresses. This thin specimen, shown in Figure 3, was used to obtain the stress-free reference d_0 neutron diffraction measurements.

Figure 3. 3013 outer container specimen cut from companion lid for stress-free reference measurements.

Neutron diffraction measurements were performed on the closure weld region of the intact 3013 outer container and the thin 3013 outer container specimen, at the same time, using polychromatic neutrons from the Los Alamos Neutron Science Center (LANSCE) accelerator at Los Alamos National Laboratory. The Spectrometer for Materials Research at Temperature and Stress (SMARTS)[7]was used to determine two strain components simultaneously. A schematic of the instrument is shown in Figure 4; incident collimation sets the size of the incident beam to 2x2 mm, and radial collimators limits the view of the detectors to a 2 mm long section of the incident beam. The detectors are fixed at plus and minus 90° to the incident beam direction, which means the scattering vectors are at plus and minus 45° to the incident beam, Q_1, and Q_2 in the figure, providing two orthogonal strain components for each orientation of the sample.

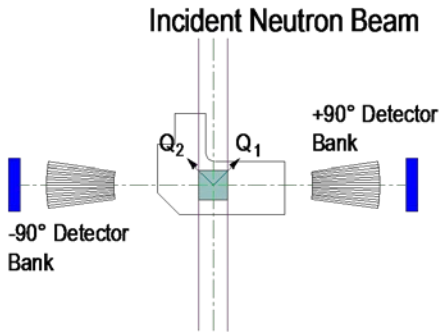

Figure 4. Schematic of the SMARTS instrument.

The lid was measured at two orientations relative to the neutron source and detector. The first orientation determined radial and axial strain and a second orientation determined hoop and off-axis strain. The off-axis strain was not used in the stress calculations, but due to excessive path lengths it was necessary to tilt the cylinder axis while measuring the hoop strains to minimize beam attenuation. Figure 2 above shows the location on the container at 180° from the weld stop that was interrogated to produce the 2D neutron map. When investigating welded samples it is also important to determine any chemistry-induced lattice parameter changes caused by the welding, and d_0 measurements were performed at several locations in the weld and in the base metal of the lid. Figure 5 is the mapping grid showing the measurement locations.

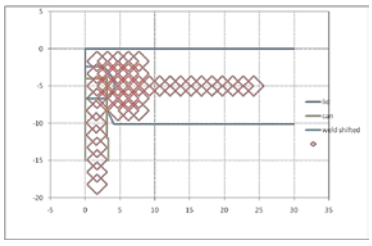

Figure 5. Mapping grid used for the neutron studies showing the measurement locations. The diamonds are a 2-D outline of the 2X2X2 mm^3 volume used for spatial averaging.

The diamonds shown in Figure 5 are a 2-D outline of the 2×2×2 mm^3 volume used for spatial averaging of the results. The scan was extended at mid-thickness of the lid to confirm balancing compressive stresses and for comparison with contour measurements.

A 360° circumferential scan was conducted taking measurements at least every 30°. Only one orientation was measured so hoop strain and not stress was determined. A digital gauge was used to ensure the top of the cylinder was running true during the rotation to within ±25 micron.

Rietveld refinement was used to fit measured intensity to a crystal structure model and obtain average lattice constants. Strain was then determined from these "stressed" lattice constants and the measured lattice constants of the unstressed material. Error bars based on peak-fit uncertainties for the strain were 15-30 με for axial, 10-40 με for radial and 20-110 με for hoop, resulting in stress error bars of 5-15 MPa, 5-15 MPa and 5-30 MPa for axial, radial and hoop stresses, respectively.

3013 Outer Container Contour Method Measurements

The following is a summary of the contour method measurement as it was applied here.

1. Cut the lid off of the container. The cut was far enough from the weld to have minimal effect on the stresses near the weld.
2. Cut specimen along measurement plane (wire EDM).
3. Measure deformed shape of both cutting surfaces.
4. Average displacements from both cutting surfaces.
5. Filter noise from average displacements by fitting to a smooth analytical surface.
6. Construct finite element model of the specimen.
7. Apply smooth displacement surface to finite element model as a displacement boundary condition.
8. Solve for equilibrium to get an estimate of the initial residual stress

The contour method was used to produce a two-dimensional map of the residual hoop stress in the same 3013 outer lid used for neutron diffraction measurements (H003085). Prior to completing the contour measurement, the lid was sectioned from the rest of the container by cutting at 16 mm from the top surface of the lid. Contour data was obtained by cutting through the center of the container lid along the 0° to 180° plane where 0° is the weld stop location. (Figure 6)

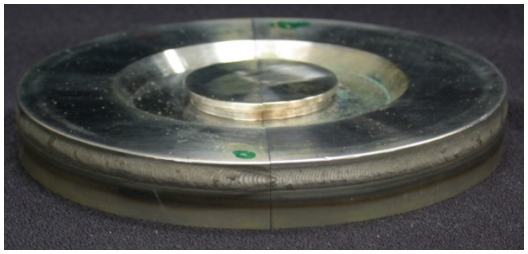

Figure 6. 3013 outer container lid after being cut in half.

The 180° location was the same as that of the location of initial neutron measurements shown in Figure 2.

3013 Outer Container Results and Discussion

Residual stresses determined from the neutron scattering results on the 3013 outer container are illustrated in Figure 7.

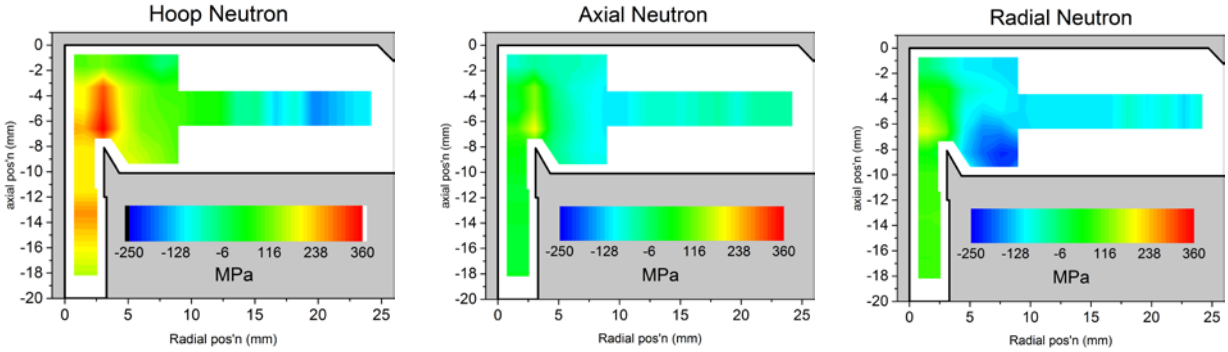

Figure 7. Contour plot of stresses in a 3013 outer container measured using neutron scattering.

Hoop stresses in the weld region were the largest magnitude stresses determined in the container. Maximum stresses in the weld region were subsurface hoop stresses of approximately 360 MPa located 3.2 mm from the outer wall and 6.7 mm from the top of the lid. Axial stresses of approximately 200 MPa and radial stresses up to approximately 180 MPa were also observed in the closure weld region. Hoop stresses up to ~ 270 MPa were observed in the container wall below the weld. Plots of the measured residual stresses along a horizontal line at the mid thickness of the lid and a vertical line down through the can wall are shown in Figure 8.

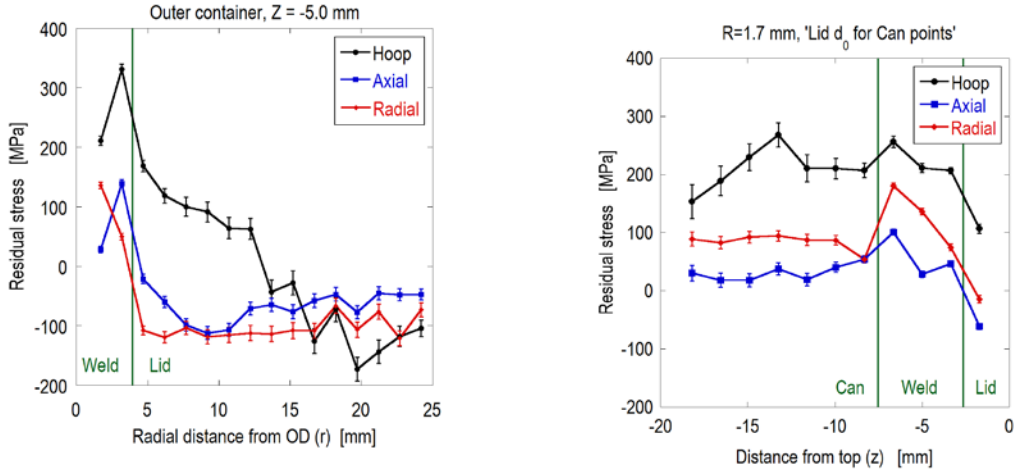

Figure 8. Line plot of residual stresses measured (a) through the lid at the weld location as a function of distance from the outer wall, (b) down through the can wall as a function of distance from the top surface.

The former plot shows that modest balancing compressive stresses were also observed in the lid and the latter show tensile hoop stresses in the can wall consistent with the press fit of the lid into the can prior to welding.

Accurate unstressed lattice spacing d_0 is key for getting accurate stresses but is difficult to obtain in welded parts. The d_0 values change with changes in alloy chemistry and other material changes. Figure 9 shows an etching of the weld region from the d_0 specimen shown in Figure 3.

Figure 9. Etching of the weld region of the d_0 specimen showing two of the sampling volumes for the neutron measurements.

Two of the sampling volumes for the neutron measurements are sketched in Figure 9. One of the sampling volumes overlaps the weld region and the heat-affected zone. Other sampling volumes, not shown, include the heat-affected zone or the base material or some of both. The d_0 can be expected to vary in the weld region. A single d_0 value in the container lid was measured for the base material and two d_0 values were measured within the weld approximately at the locations shown in Figure 9.[*] For locations within the weld, the d_0 used was determined by interpolation between the two measured d_0 values based on the relative location of the actual measurement points and the location of the d_0 points. The difference in d_0 values from weld and base material is equivalent to a strain difference of about 500 με, corresponding to about 100 MPa, so there is potential for large errors if the d_0 values used are not determined accurately. Note also that d_0 was only measured in one orientation, giving values for radial and axial directions but not hoop. The d_0 measured for the axial direction were also used for hoop measurements because both were measured in detector bank 1.

Additional measurements were obtained to determine the variation in strain as a function of location on the circumference of the container. The location of maximum hoop stress

[*] Detailed analysis of all the d_0 measurements showed the d_0's measured in the can wall were far from the d_0's measured in the lid. As both are 316L they should have the same stress-free lattice parameter. The can d_0 was very close to the d values for the weld material, which physically does not make sense. Therefore the d_0 measured in the lid was used for calculating all strains outside the weld.

in the weld, ~3mm inward from the outer wall, was used. See the yellow diamond in Figure 10 below.

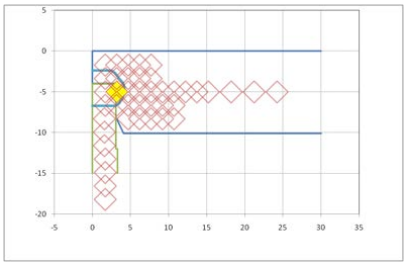

Figure 10. Location used for circumferential scan of container.

Results of the 360° circumferential neutron diffraction scan are shown in Figure 11.

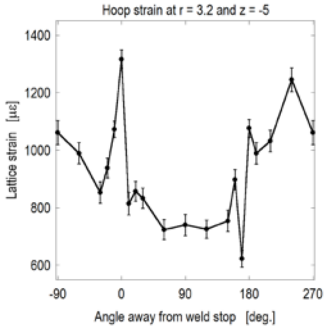

Figure 11. Hoop Strain in 3013 outer container as a function of angular distance from the weld stop.

Hoop strain varied from a maximum of 1320 microstrain near the weld stop to a minimum of 620 microstrain approximately 170° away from the weld stop. The general trend for the hoop strains is a slow wave with high point around 240° and a low point in the region around 60-120°, but with significant spikes just before 0° and just before 180°. The spike just before the weld stop is expected as that was the last material to cool from the welding process, and thus it should end up in tension but the drop at 170° is not so easy to explain. It could be related to the tack-welds done prior to the continuous weld but this seems unlikely since consistent behavior at each tack weld location would be expected. The general wave in the hoop strain could be related to the change in weld speed as described above.

Residual hoop stress results obtained using the contour method are shown in Figure 12. The left of the figure is the 180° location (same measured by neutron) and the right of the figure is 0° (weld stop).

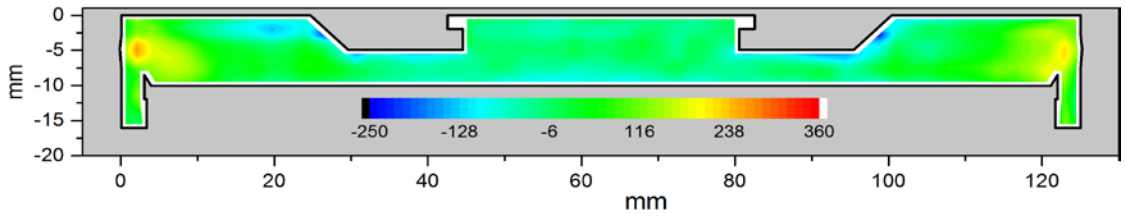

Figure 12. Residual Hoop Stresses in a 3013 outer lid obtained using the contour method.

Maximum hoop stresses of approximately 260 MPa were observed subsurface in the closure weld region.

Figure 13 compares the residual hoop stresses measured in the lid of the intact 3013 outer container using neutron diffraction with those obtained on the lid section using the contour method using the same color scale.

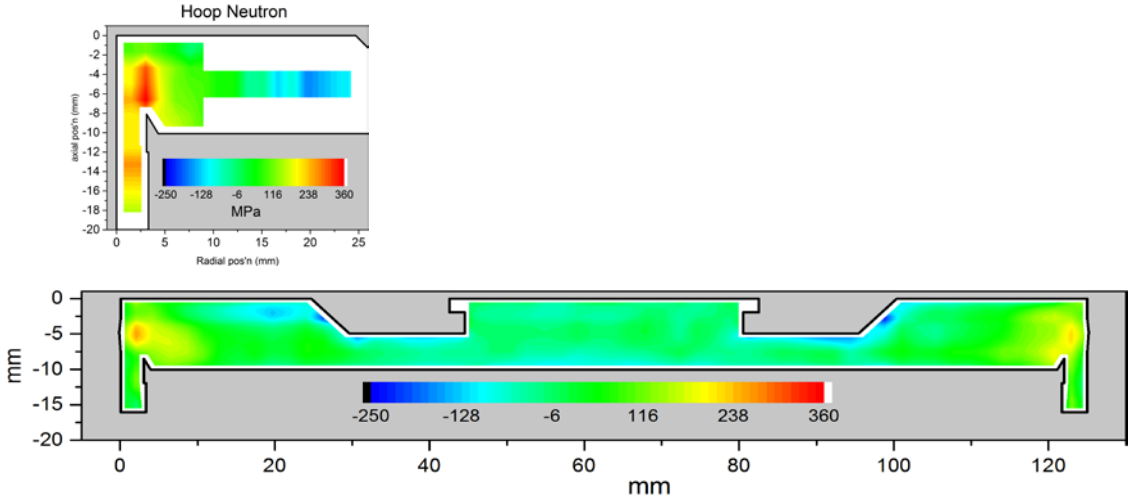

Figure 13. Residual Hoop Stress in a 3013 Outer Container lid: Top: Neutron Diffraction: Bottom: Contour.

Hoop stresses in the wall region measured in the cut off container using the contour method were significantly lower than stresses determined in the wall of the intact container using neutron diffraction. Hoop stresses in the wall of the container may have relaxed during the trimming process that occurred prior to obtaining contour data. No correction was made for stress relaxation due to trimming in the reported contour data because finite element simulations indicated the relaxation of hoop stress due to the cut would be insignificant. However, significant axial strain relaxation due to trimming was observed in the 3013 inner container trimmed to 38mm. (See Table 2 below.)

Errors are possible with the contour method. Like other relaxation methods, the contour method assumes that the stresses relax elastically during the cutting. Therefore, local plasticity could cause errors[8]. Also, the effective cut width can change as the part deforms during cutting causing a "bulge" error.[9] Both of these error sources increase with higher magnitude stresses and tend to cause an overestimation of residual stresses, which does not explain the lower stresses measured by contour relative to neutron.

Both techniques determined that the maximum hoop stresses in the container were subsurface in the closure weld region. However, neutron scattering results obtained at the second sampling volume approximately 3mm from the outer surface, had significantly higher hoop stresses (360 MPa) than that observed by the contour method (260 MPa). Figure 14a compares hoop stresses measured using neutron diffraction and the contour method as a function of distance from the outer wall. The approximate locations of the measurements are shown in Figure 14b.

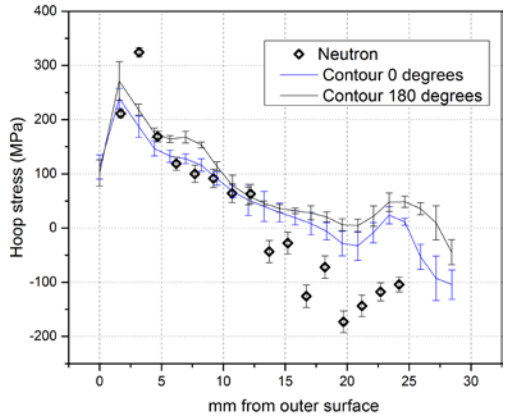

Figure 14a

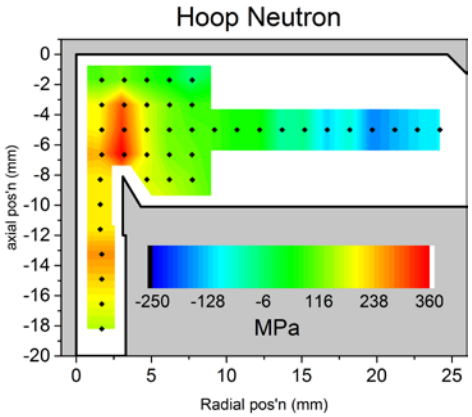

Figure 14b

Figure 14 (a). Hoop Stresses vs distance from outer surface measured using neutron diffraction and the contour method **14(b).** Location of data for plot 14(a).

Figure 14a shows the variation of hoop stress along a horizontal line through the lid of the container as measured by both neutron diffraction and contour methods; starting at the weld location on the outer diameter and going towards the center of the lid. The overall trends agree well; tension close to the outer surface changing to compression about 15 mm into the lid. The neutron diffraction data does show a higher scatter; especially the point at approximately 3 mm from the outer diameter which shows significantly higher stress level than for the contour method. This location is right on the edge of the weld region (See Fig. 9), and thus in a region of possible high gradients in chemistry. These gradients can cause additional non-strain related shifts in the lattice parameter leading to larger error bars for the determined strain and stress. Further into the lid, in the compressive region, the neutron diffraction data shows higher scatter and values somewhat lower than the contour method.

The lack of agreement between the contour and neutron results is somewhat discouraging. The most likely explanation seems to be d_0 errors in the neutron measurements, and this is precisely the reason that many industries that care about welding stresses, such as nuclear power, increasingly use the contour method. However, we cannot be sure which measurements are more accurate. The most prudent approach is to take the worst case, in this case the higher tensile stresses measure by neutron diffraction, to use with failure analyses.

III. 3013 INNER CONTAINER STUDIES

Residual stress measurements were performed on two SRS/Hanford inner containers (S/N: H5107 and H5117) and a RFETS/LLNL inner container.

SRS/Hanford 3013 Inner Containers

SRS/Hanford inner containers and lids were of the bagless transfer design and made from 304LSS with low sulfur content. Precision flow forming, a cold metal forming process where a preform is extruded over a rotating mandrel to produce a rotationally symmetrical hollow component, was used to fabricate the containers. There were no fabrication welds in the container body. There was a GTAW autogenous closure weld.[3] The containers were prototype containers welded at SRS using the GTAW technique later implemented at Hanford. Unlike most of the inner containers in use for storage of nuclear material, the inner surfaces of these prototype containers were blasted with walnut shells to roughen the surfaces prior to machining and welding. The bottoms of the containers were removed prior to completing any measurements to ensure there was no contamination in the containers. Boiling $MgCl_2$ SCC susceptibility studies identified the inner container closure weld region (ICCWR) and the container bottom as susceptible locations for SCC in SRS/Hanford 3013 inner containers. SCC cracking occurred more rapidly in the ICCWR than the bottom indicating this is the region most susceptible to SCC. In addition, corrosion observed during destructive examination of Hanford/SRS 3013 inner containers used to store nuclear material showed similar or worse corrosion in the ICCWR than in the rest of the container.[10]

IIIA. SRS/Hanford Inner Container H5107

Experimental Methods

Residual stresses in the SRS/Hanford inner container H5107 were determined using incremental hole drilling and the contour method. Contour and hole drilling measurements and data analysis were performed by Hill Engineering, LLC.

Incremental Hole Drilling Measurements

Incremental hole drilling was used to measure residual stresses at 8 locations in the ICCWR of SRS/Hanford inner container H5107. The incremental hole drilling method[5] is a measurement technique for determining in-plane residual stress versus depth from the material surface. In the hole drilling method, a hole is incrementally extended into a body containing residual stress. The strain released with each increment in hole depth is measured using a strain gauge rosette placed around the hole. The measured strains versus hole depth data are used to calculate the residual stress that was initially in the part through an elastic inverse solution. Each hole was drilled in 0.05 mm (0.002 inch) increments to a final depth of 1 mm (0.040 inch). The 0° location was defined as the angular position of the stop location of the weld. First, two holes (HD1 and HD2) were drilled on the top of the lid at 22.5° and 220.5° to measure radial and hoop stress (Figure 15).

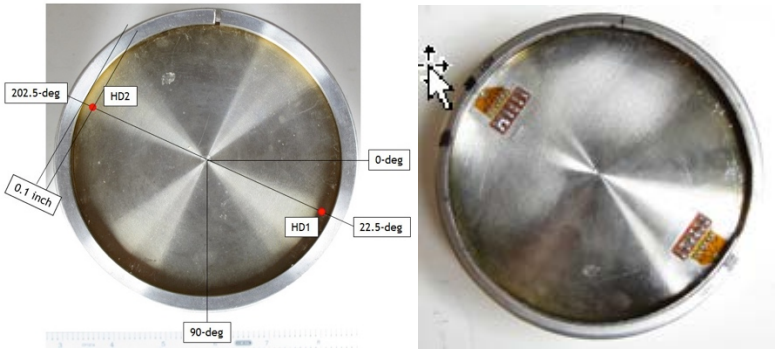

Figure 15. Photographs of hole drilling and strain gauge locations for HD1 and HD2 on the SRS/Hanford inner container lid H5017.

Prior to making additional measurements, the H5107 container wall was trimmed closer to the container lid. Four strain gauges were applied to the top of the lid and four gauges were on the wall along the 0° and 90° planes to measure strain changes during the trimming process. (Figure 16).

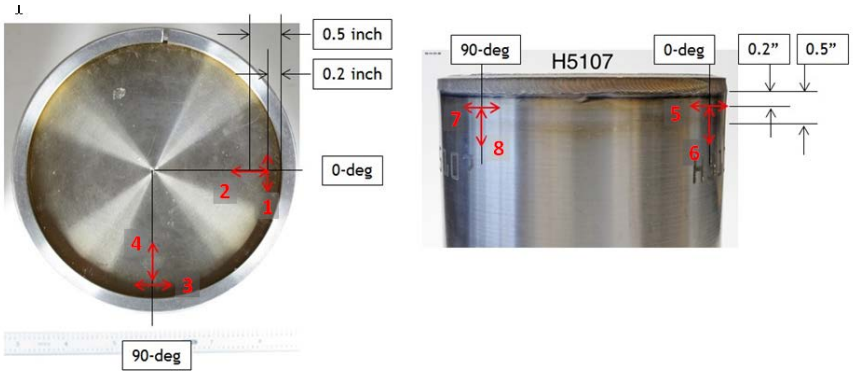

Figure 16. Photograph of container showing the location of the strain gauges during trimming of the SRS/Hanford inner container H5107.

The container was trimmed to 102 mm (4 inches) from the top of the container. Then the container was trimmed in 13 mm (0.5 inch) increments until 38 mm (1.5 inches) of wall extending down from the top of the lid remained (Figure 17).

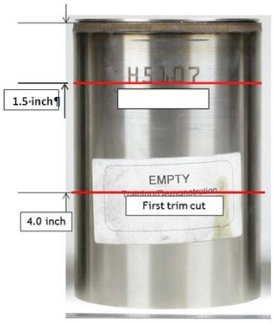

Figure 17. Photograph of container showing location of second and final trim cut of the SRS/Hanford inner container H5107.

Strains were recorded at each increment in the trimming process. The trimming was terminated when significant strain due to the trimming process was observed. The total measured strain data after the final trim are shown in Table 2 along with calculated stress values.

Table 2. Measured strain and calculated stress changes in the SRS/Hanford container H5107 by trimming.

Location	1	2	3	4	5	6	7	8
Strain Direction H=Hoop, A=Axial, R = Radial	H	R	H	R	H	A	H	A
Measured Strain (με)	0	-8	-9	+9	+8	+117	+7	+113
Stress (MPa)	0	-2	-2	+2	+2	+23	+1	+22

During trimming, the radial and hoop strain measurements on the lid (strain gauge locations 1-4) and hoop strain on the wall (strain gauge locations 5 and 7) were very low magnitude (less than 10 με). However strain measurements in the axial direction in the heat affected zone (HAZ) of the container wall (strain gauge locations 6 and 8) indicated the stress in the wall below the weld increased by approximately 20 MPa during trimming. Reported results for H5107 were not corrected for these changes.

After the H5107 was trimmed down to a total height of 38 mm, the container was cut along the 0° to 180° plane for the contour method measurement described below. Incremental hole drilling was then used to measure residual stresses at six additional locations on one of the remaining halves. The magnitude of stresses in the remaining half section that were released during the contour measurement cut were calculated. Attachment 1, *Residual Stress Data Summary for locations HD1-HD12*, Tables A2-A7, provide detailed information at the six hole drilling locations on the calculated stresses in the cut container, the stresses released by the contour cut and the total residual stress in the container prior to the contour cut (Calculated stress + Released Stress (contour cut) = Reported Stress.) Hole drilling results presented are the total residual stress corrected for the contour cut. The locations of the incremental hole drilling on one of the remaining halves are given in Figure 18.

Location	Distance below Weld (mm)	Approx. Angle	Hole Start
HD3	12.5	104°	ID
HD4	2.5	90°	OD
HD5	12.5	90°	OD
HD6	5	76°	OD
HD7	9	62°	OD
HD8	2.5	14°	OD

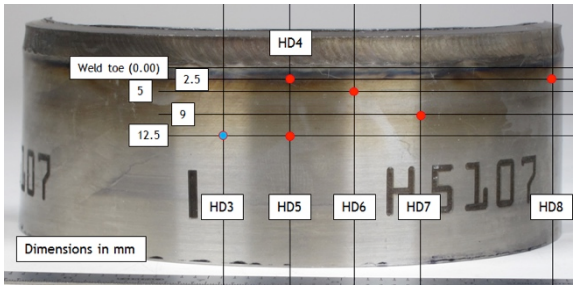

Figure 18. Table of hole drilling measurement location for HD3-HD8 and photograph showing l hole drilling measurement locations on the SRS/Hanford inner container lid section of H5107. (ID indicates hole drilling started from the inner wall and OD from the outer wall.)

Location HD3 was drilled from the inner wall outward. Hole drilling locations HD4 through HD8 were drilled from the outer wall inward. Holes were spaced approximately 12.5 mm or more apart to minimize effects from neighboring holes.

Contour Method Measurements

After the H5107 was trimmed down to a total height of 38 mm, contour measurements were obtained. The contour method was used to measure a two-dimensional map of the residual hoop stress over 3 radial planes: cutting through the center of the container lid along the 0° to 180° direction (Plane 1), cutting along the 90° direction (Plane 2), and cutting along the 45° direction (Plane 3). See Figure 19 for information on cut locations. Detailed information on the contour method may be found in Chapter 5 of reference 6.

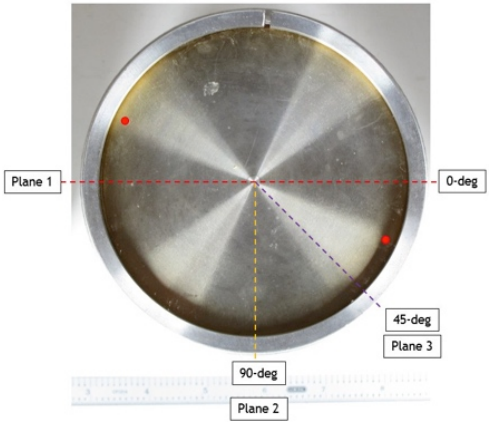

Figure 19. Photograph of Lid with Plane 1 through Plane 3 contour measurement locations 0° is defined as the weld stop of the SRS/Hanford inner container lid H5107. The top half of the container section was used for the hole drilling measurements.

Results and Discussion

Residual stresses measured in the lid of H5107 as a function of depth during incremental hole drilling are shown in Figure 20.

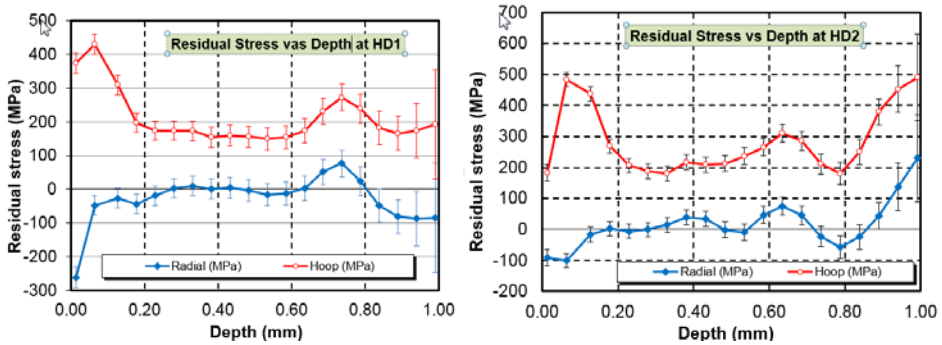

Figure 20. Hole Drilling method measured residual stress vs. depth into the lid for location HD1 and HD2 in the SRS/Hanford inner container H5107.

For all incremental hole drilling results, uncertainty increased with increasing hole depth. Hoop stresses above 400 MPa were measured near the lid surface and tend toward zero with increasing distance from the surface. Radial stresses are compressive at the lid surface and tended toward zero with increasing depth.

Hoop stress results from incremental hole drilling at locations for HD3-HD8 taken after the SRS/Hanford inner container H5107 was trimmed and cut in half are summarized in Figure 21.

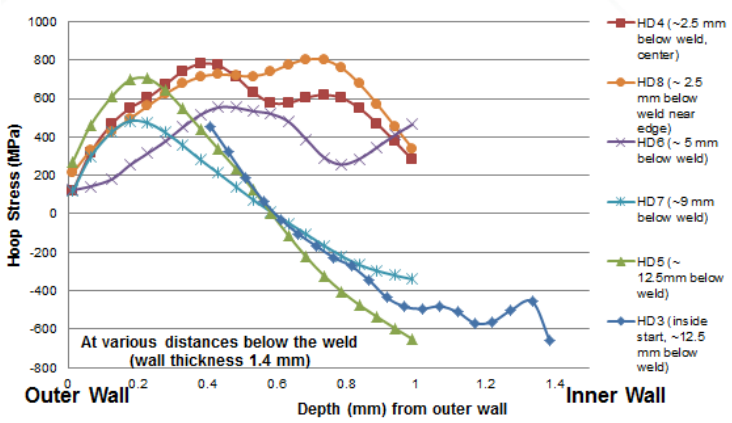

Figure 21. Graph of ICCWR hoop stresses at various distances below the weld toe in H5107.

Hoop stresses in the wall varied significantly both as a function of distance below the weld toe and distance through the wall. The highest observed hoop stresses were approximately 800 MPa located near the center of the wall 2.5 mm below the weld toe (HD4 and HD8). Stresses of this magnitude are higher than the 210 MPa yield strength of 304L SS that is not work hardened. However, both flow forming and welding cause work hardening and explain the ability of the material in this container to support such high residual stress in this region. At 2.5 mm and 5 mm below the weld, only tensile hoop stresses were observed to the depth that was measured. At 9 mm and 12.5 mm below the weld stresses were tensile near the outer wall but moved to compressive near the center and toward the inner wall. This result is consistent with the pattern of stress corrosion cracks observed in the ICCWR of SRS/Hanford inner containers during the boiling $MgCl_2$ experiment conducted by Mickalonis et. al[2]. When the inner wall was exposed to the boiling $MgCl_2$ solution, vertical cracks extended from the weld toe to approximately 5-9 mm below the weld toe (Figure 22). This closely matches the region where tensile hoop stresses found near the inner surface transitioned to compressive stresses. There was reasonable agreement between the HD3 and HD5 stress vs. depth results obtained by drilling from opposite sides of the wall at 12.5 mm below the weld toe.

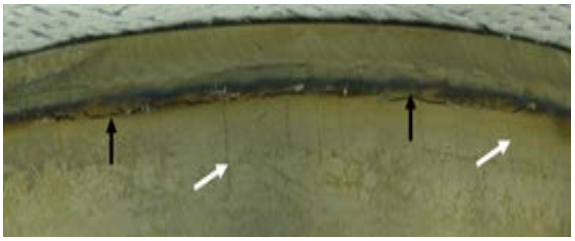

Figure 22. Exterior of ICCWR after exposure to boiling $MgCl_2$ has cracks parallel to the weld due to axial stresses and numerous cracks 5-9 mm long perpendicular to the weld due to hoop stresses.

Results for axial stresses determined from incremental hole drilling of SRS/Hanford inner container H5107 after trimming and cutting are shown in Figure 23.

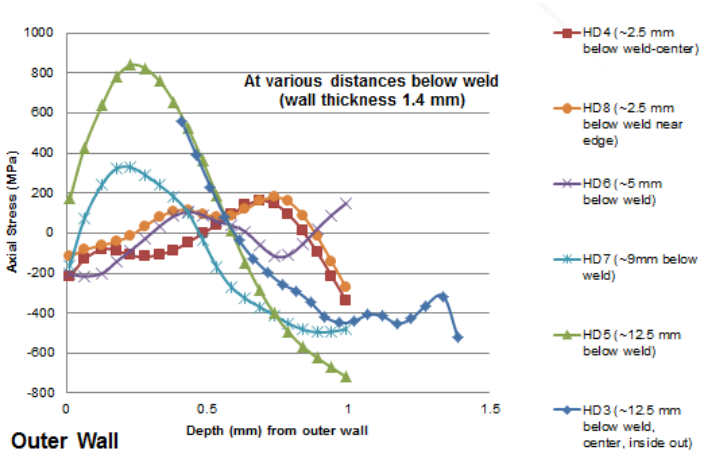

Figure 23. Graph of ICCWR Axial stresses at various distances below the weld toe in H5107.

Axial stresses, shown in Figure 23, also varied significantly both as a function of distance below the weld toe and distance through the wall. They reached a maximum tensile value of approximately 800 MPa near the outer surface at 12.5 mm below the weld (HD5). Close to the weld toe (HD4 and HD8) the measured residual axial stress did not exceed 200 MPa. As with hoop stress, there was good agreement between the results obtained drilling 12.5 mm below the

weld toe from the inside outward and from the outside inward where there was overlap in depth coverage (HD3 and HD5).

A contour plot of the residual hoop stress in the SRS/Hanford container H5107 determined from the Plane 1 cut is shown in Figure 24.

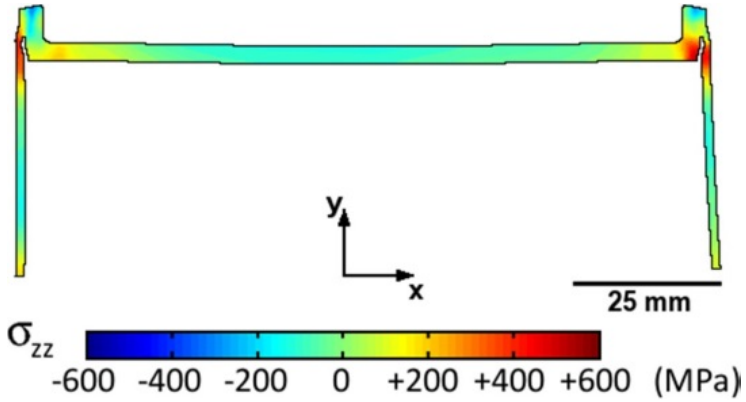

Figure 24. Contour plot of hoop stress for Plane 1. The right side of the plot corresponds to the weld start/stop.

This plot indicates that the higher magnitude residual stresses both in the wall and lid were concentrated near the weld. The residual stress near the weld stop location (0°, right side) was slightly higher in magnitude than the residual stress 180° away.

A contour plot of the released residual stress (maximum principal component) throughout the entire lid section as a result of the Plane 1 cut is shown in Figure 25.

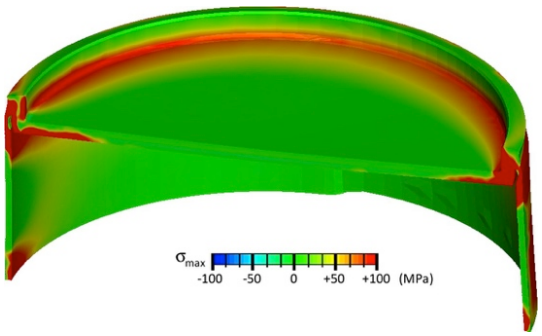

Figure 25. Contour plot of hoop stress **released** throughout the SRS/Hanford inner container as a result of the Plane 1 cut.

Hole drilling results reported above (Figures 20, 21 and 22) are corrected for these released stresses. The magnitude of the hoop stress released varied significantly with distance below the toe weld as well as distance from the Plane 1 cut. Calculated hoop released stress at several locations corresponding to those probed by hole drilling are summarized in Table 3.

Table 3. Location and Released Hoop Stress from Plane 1 Cut for hole drilling locations HD3-HD8 in container H1057.

Hole	Distance below Weld (mm)	Approx. Angle	Hole Start	Hoop Stress Released (MPa)	Axial Stress Released (MPa)
HD3	12.5	104°	ID	16-19	(-26) - 9
HD5	12.5	90°	OD	13	(-33)- (-1)
HD4	2.5	90°	OD	91-106	100 - 52
HD8	2.5	14°	OD	222-225	124 - 144
HD6	5.0	76°	OD	71-86	87-72
HD7	9.0	62°	OD	45-48	48 - 45

Additional data on stress releases may be found in Attachment 2, *Hoop stresses as a function of distance down the wall in H5107 container.* The magnitude of the released hoop and axial stress decreased with increasing distance from the weld toe. Released axial stresses were compressive at 12.5 mm below the weld. The magnitude of the release hoop stress also decreased with increasing distance from the Plane 1 cut (0° and 180°). The largest release of hoop (222-225 MPa.) and axial (124-144 MPa) stresses occurred at the location of HD8 at 14° from Plane 1. In contrast, released hoop (92-106 MPa) and axial stresses (100-52 MPa) were much lower at the location of HD4 which was 90° from the cut.

Contour plots of the measured, released (from Plane 1 cut) and total hoop stress (measured plus released) for the Plane 2 cut are shown in Figure 26.

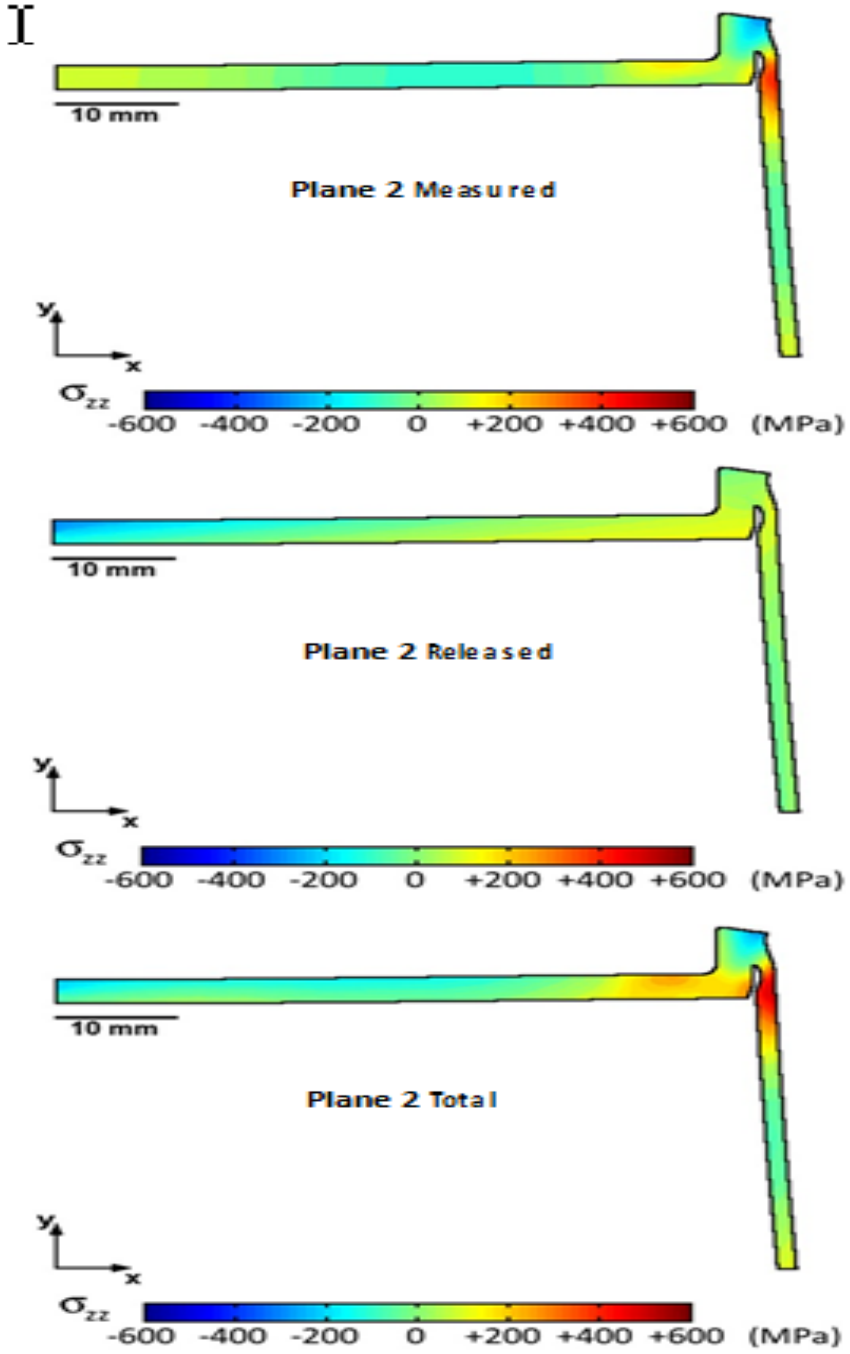

Figure 26. Contour plot of hoop stress for Plane 2.

Further sectioning of the lid resulted in additional stress releases. Contour plots of the hoop stresses for Plane 3 including corrections for stress release from the Plane 1 and Plane 2 cut, are shown in Figure 27.

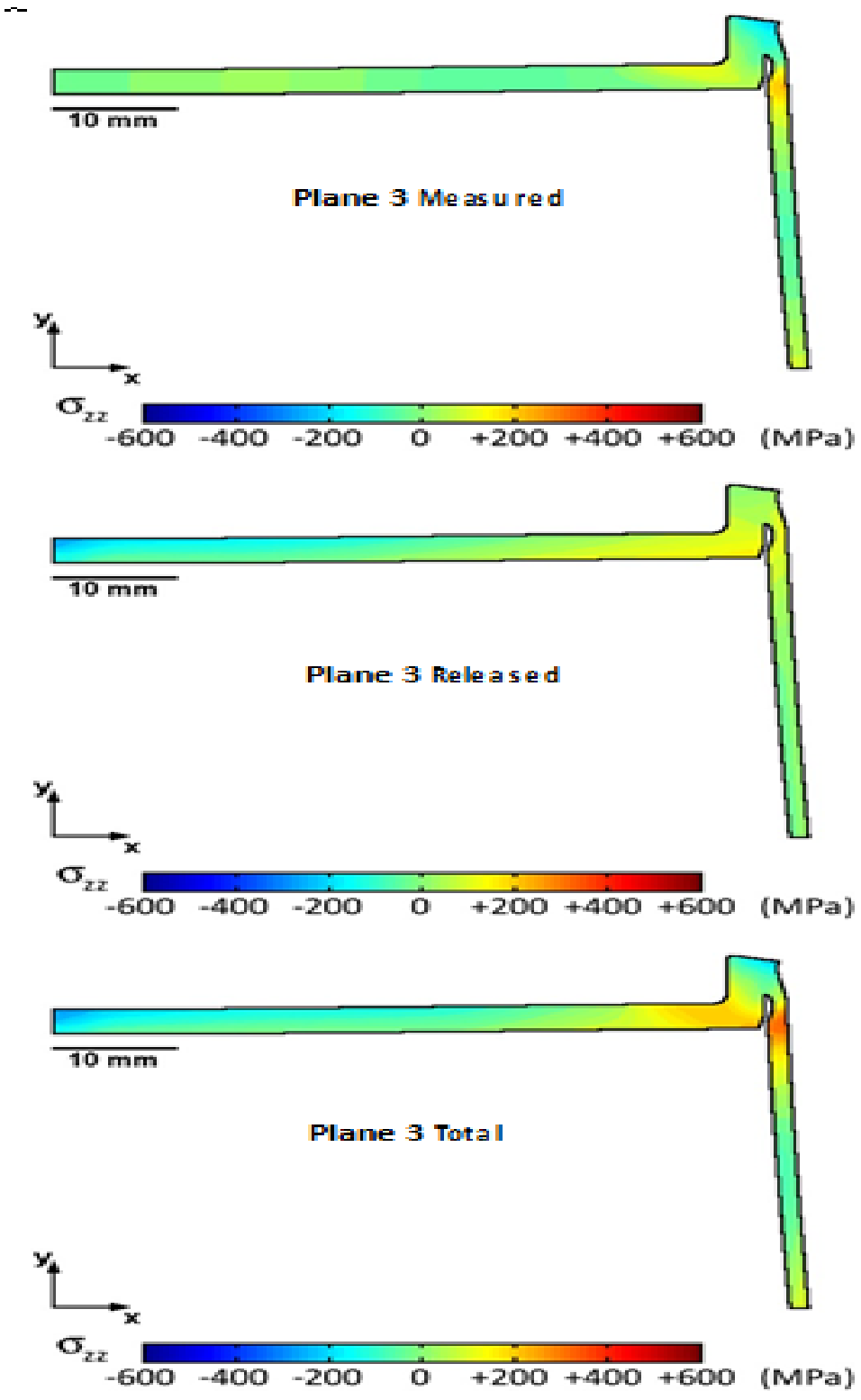

Figure 27. Contour plot of hoop stress for Plane 3.

All H5107 container contour plots indicate that the highest magnitude residual hoop stress was concentrated in the wall below the closure weld. Line plots of the residual stresses down the container wall are shown in Figure 28. Calculated hoop stress results are summarized in Attachment 2, *Hoop stresses as a function of distance down the wall in H5107 container*.

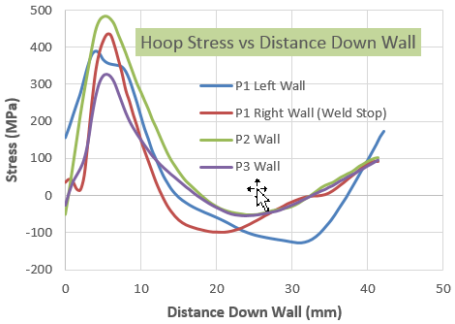

Figure 28. Line plots of residual hoop stressed down container H5107 wall.

Figure 28 indicates that the maximum residual hoop stress near the weld varied from 300 to 480 MPa, depending on the location of the cut around the circumference of the lid.

IIIB. SRS/Hanford Inner Container H5117

Experimental Methods

Incremental hole drilling was also used to measure residual stresses at 4 locations in the wall of container H5117. Each hole was drilled in 0.05 mm increments to a final depth of 1.0mm. The 0° location was defined as the angular position of the stop location of the weld (Figure 29).

Figure 29. Photograph of Lid of 3013 inner container H5117 showing two large weld defects.

Information on the location of the holes is shown in Figure 30.

Location	Distance below Weld (mm)	Arc Length from 90° ref (mm)	Approx. Angle	Hole Start
HD9	2.5	19	109°	OD
HD10	1.0	19	71°	OD
HD11	2.5	6	96°	ID
HD12	2.5	6	84°	ID

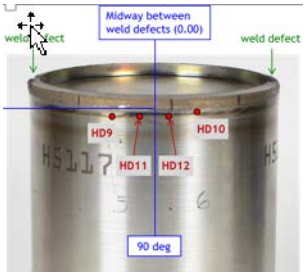

Figure 30. Table of hole drilling measurement locations (left) and photograph of approximate hole drilling measurement location on H5117.

First, HD9 and HD10 were drilled from the outer wall inward on the container with the intact lid. A section of the lid was then removed in a two-step process (Figure 31) to enable hole drilling on the inner wall of the container close to the weld.

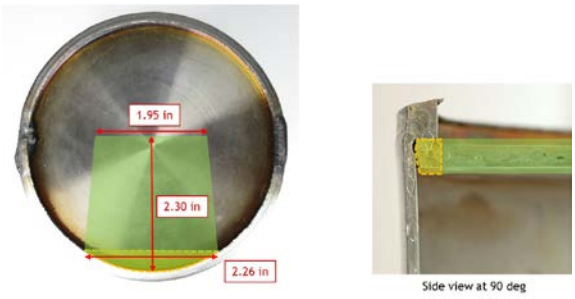

Figure 31. Photograph of Sectioning cuts; cut hole in lid (left) and remove rest of lid lip to expose inner wall.

Strain gauges were placed on the container outer wall prior to the cutting process. (Figure 32).

Location	Distance below weld (mm)	Arc Length from 90° ref (mm)	Approx.. Angle	Hole Start
Gauge 1	2.5	6.4	96°	OD
Gauge 2	2.5	6.4	84°	OD

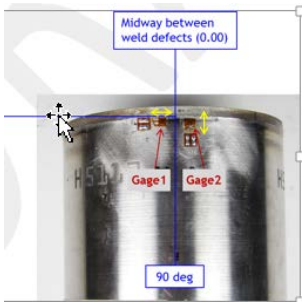

Figure 32. Table of strain gauge measurement locations (left) and photograph of container H5117 strain gauge placement and measurement direction for the sectioning cuts (right).

The measured strain values near the location of interest (strain gauge locations 1 and 2) recorded during the sectioning steps of the experiment are shown in Table4.

Table 4. – Strain changes due to removal of a section of the lid.

	Gauge 1 (Hoop) [με]	**Gauge 2 (Axial) [με]**
Strain change from cutting hole in lid	-1084	-255
Strain change from removing lid lip	394	173
Total strain change (final minus initial)	-690	-82

Assuming that the gauges are oriented in the direction of the principal strains, the released stress due to sectioning would constitute approximately -150 MPa in the hoop direction and -60 MPa in the axial direction. This means that the initial residual stress prior to removing a section of the lid would have been more tensile by approximately 150 MPa in the hoop and 60 MPa in the axial

directions at the outer diameter of the canister. These values are provided for reference. The reported measured residual stresses have not been corrected for the sectioning process.

After the lid sectioning, HD11 and HD12 were drilled from the inner wall outward (Figure 33).

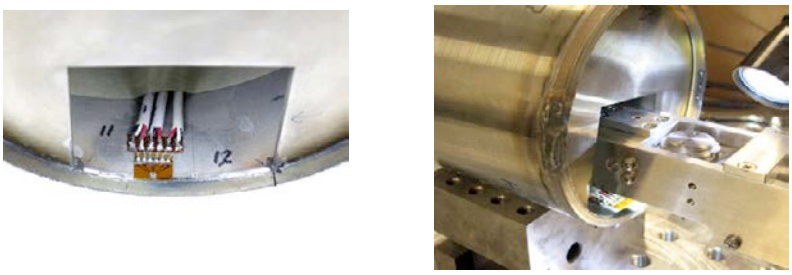

Figure 33. Photographs of SRS/Hanford inner container prior to drilling HD11 and HD12.

Hoop stress results of the HD9 – HD12 measurements are shown in Figure 34.

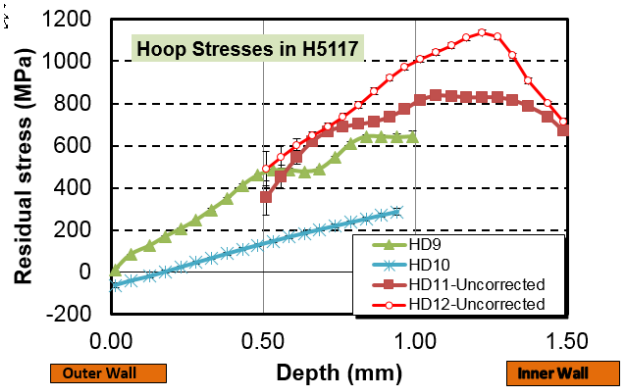

Figure 34. Line plot of hoop stresses measured in H5117 using incremental hole drilling.

Hoop stresses of approximately 10 MPa were present on the outer wall of the SRS/Hanford inner container H5117 at a position 2.5 mm below the weld toe (HD9). Stresses increased steadily with depth over the full depth range of the measurement. Similarly increasing but significantly smaller hoop stresses were observed 1 mm below the weld toe (HD10). Hoop stresses of approximately 690 MPa were measured on the inner wall near the weld (HD11 and HD12) and reached maximum values above 800 MPa 0.3 mm below the inner surface before declining with depth. There was reasonable agreement in the measured stresses by outside-in (HD9) and inside-out drilling (HD11 and HD12) in wall regions where the measurements overlapped.

The residual axial stresses measured in container H5117 using incremental hole drilling are shown in Figure 35.

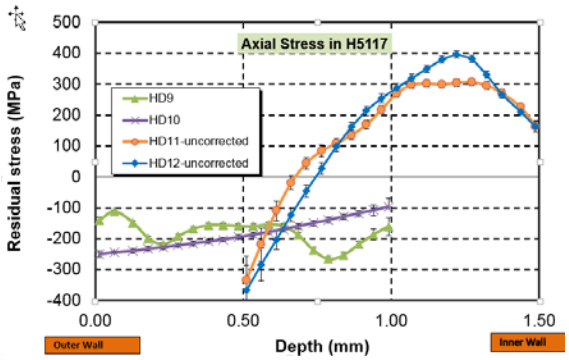

Figure 35. Plot of Axial Stresses measured in H5117 using incremental hole drilling.

Fairly constant compressive axial stresses between -100 and -300 MPa were found over the full 1 mm depth of the hole drilling measurements from the outer wall of container H5117 at 2.5 mm below the weld toe (HD9) and 1 mm below the weld toe (HD10). Measured values for HD9-HD10 are detailed in Attachment 1, Table A8. Results were significantly different for the data obtained from the inner wall outward (HD11 and HD12). Axial stresses of approximately 160 MPa were found at inner wall surface, rose above 300 MPa from 0.2 to 0.5 mm below the surface, and then decreased to zero or compressive values at and beyond the midpoint of the wall. The agreement between inward and outward hole drilling in the overlap region is not as good as in other cases discussed above.

Comparison of Hole Drilling and Contour Results on SRS/Hanford Inner Containers in the ICCWR

Table 5 below summarizes information about the hole drilling or the SRS/Hanford inner containers. Full results for HD1-HD12 are summarized in Attachment 1.

Table 5. Summary information about the hole drilling for SRS/Hanford inner containers.

SRS/Hanford Inner Container	ID	Location	Distance below Weld Toe (mm)	Approx. Angle from weld stop	Hole Start	Lid Section
H5107	HD2	Lid	N/A	N/A	Top	Entire
H5107	HD3	Lid	N/A	N/A	Top	Entire
H5107	HD3	Wall	12.5	104°	ID	Half
H5107	HD5	Wall	12.5	90°	OD	Half
H5107	HD7	Wall	9.0	62°	OD	Half
H5107	HD6	Wall	5.0	76°	OD	Half
H5107	HD4	Wall	2.5	90°	OD	Half
H5107	HD8	Wall	2.5	14°	OD	Half
H5117	HD9	Wall	2.5	109°	OD	Entire
H5117	HD10	Wall	1.0	71°	OD	Entire
H5117	HD11	Wall	2.5	96°	ID	Entire Wall Partial lid
H5117	HD12	Wall	2.5	84	ID	Entire Wall Partial lid

Figure 36 summarizes the results obtained by incremental hole drilling and contour measurements on SRS/Hanford inner containers at 2.5 mm below the toe weld in the ICCWR.

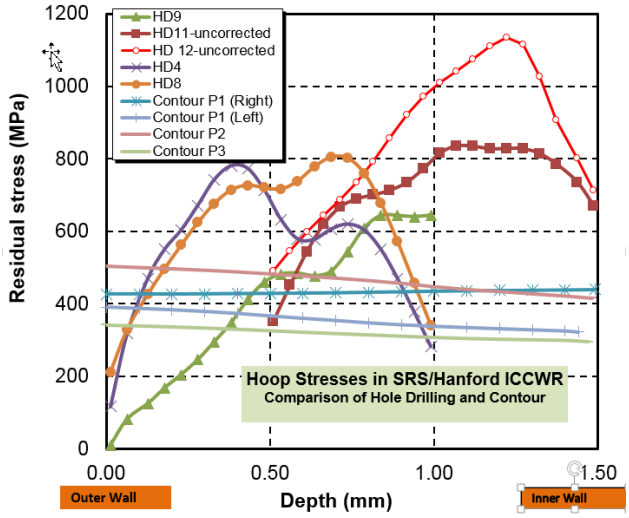

Figure 36. Comparison of total hoop stress for contour measurements (P1, P2 and P3) and hole drilling measurements (HD4, HD8, HD9, HD11 and HD12) at 2.5mm below the weld toe in SRS/Hanford inner containers.

Contour measurements appear to have sufficient spatial resolution only to provide average stress values across the thickness of the IC wall. Though hole drilling results have better resolution of stress variation with depth, the differences between the traces in Fig. 36 illustrate that there are significant variations in results. For example there was a 200 MPa variation in the residual hoop stress for HD4 and HD8 (H5107) and HD9 (H5117) measured at the outer wall of the containers. HD4 and in particular HD8 have increased uncertainty due to corrections applied because measurements were taken on half of a lid. HD11 and HD12 have increased uncertainty because these measurements are uncorrected for removal of part of the lid. Residual stress on the inner wall of the container in the ICCWR is of particular interest since this is the area where pitting corrosion is expected to occur. Contour and uncorrected incremental hole drilling measurements indicate large tensile hoop stresses (~400MPa and ~ 700MPa respectively) are present in this region at 2.5 mm below the weld toe.

IIIC. RFETS/LLNL INNER CONTAINER STUDIES

Residual stress was also determined in a RFETS/LLNL inner container #R200124. The container was a BNFL inner container and lid made from ASTM A240 316 SS. A hollow plug was press fit into the inner container and a laser closure weld was performed. There were no fabrication welds in the container body.[3] No boiling $MgCl_2$ studies were conducted on an RFETS/LLNL inner container.[2]

Contour Measurements

The contour method was used to measure residual hoop stresses in a RFETS/LLNL inner container lid. The container lid was first trimmed to a height of approximately 19 mm to ensure

a better cut during the contour measurement cutting process. Figure 37 is a photograph of the contour measurement cutting process for the RFETS/LLNL inner container lid using a Mitsubishi SX-10 EDM with a 100 μm diameter brass wire on skim cut setting to avoid inducing stress.

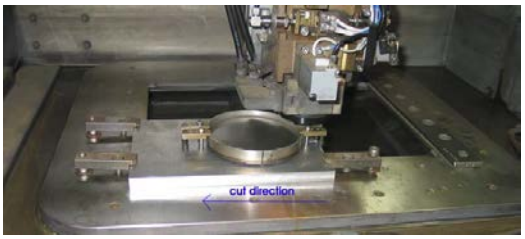

Figure 37. Photograph of EDM (wire) cut in RFETS/LLNL inner container lid for contour measurements.

Results of hoop stresses measured in the laser welded RFETS/LLNL inner container are shown in Figure 38. No corrections were made for stresses released during the trimming process.

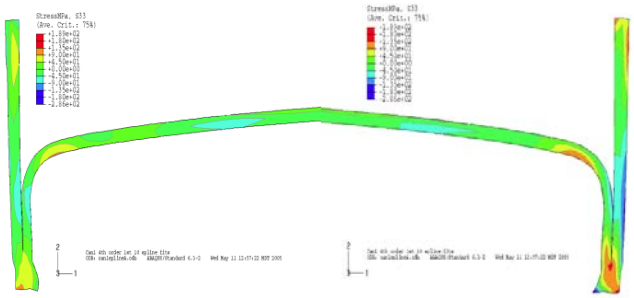

Figure 38. Hoop stresses in an RFETS/LLNL container measured using the contour method.

The maximum observed residual stress was approximately 180 MPa in the weld region. Similar stresses were also observed on the outer surface in the bend region of the lid. The maximum observed residual stress, approximately 180 MPa, was significantly less than the 480 MPa observed in the GTAW SRS/Hanford inner container.

IV. TEARDROP STUDIES

Residual stresses were measured in 304L SS teardrop samples. These samples were fabricated by bending a coupon with an approximate wall thickness of 1.3 mm around a mandrel and welding the ends together to hold them in place and lock in the high residual stress from the bending. Each teardrop contained an autogenous weld in the apex (center of the bent region) that was added to the flat specimen prior to bending. This weld results in a sensitized microstructure in the heat affected zone of the weld. The weld was added so that the teardrop specimens closely simulated the condition of the metal (HAZ) in 3013 container weld regions.[3] Boiling $MgCl_2$ SCC susceptibility studies produced through-wall cracking near the autogenous weld at the apex but outside its heat-affected zone (Figure 39).[2]

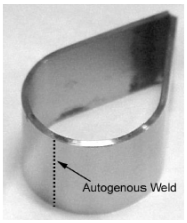

Figure 39. Photograph Teardrop Sample.

Experimental Method

A "split and slit" technique was employed to measure the residual stresses in a teardrop. The teardrop was initially split at the closure weld to release the bending moment (Figure 40). The deformation was measured and used to calculate the bending stress that had been present before the split.

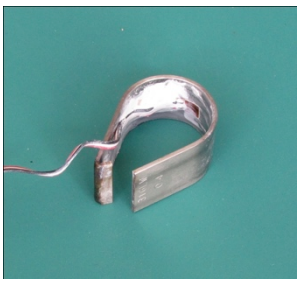

Figure 40. "Split" 304L W-02 Teardrop.

Incremental slitting[6] using EDM wire cutting was then used to measure the remaining stress in the teardrop. A strain gauge was placed on the inner wall of the teardrop prior to slitting. Slitting measurements were only obtained to a cut depth of 0.16mm Figure 41 shows the location and depth of the slit.

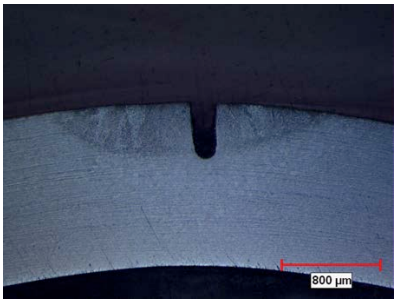

Figure 41. Weld region of teardrop after slitting

Results and Discussion

Results of the residual stress measurements in the "split and slit" on a 304L welded teardrop are illustrated in Figure 42.

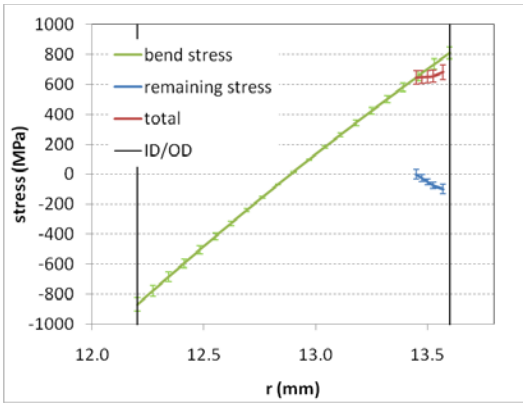

Figure 42. Plot of Stresses vs teardrop radius.

The major component of the stress in the teardrop was the bending stress released when the teardrop was split. Slitting showed that a small compressive stress remained at the outer surface after splitting. There was significant uncertainty in the slit depth because of the curvature of the surface but this does not change the conclusion. Residual stress was calculated from a superposition of the two stress components. Calculated residual stress in the apex region of the teardrop on the surface was 680 ± 50 MPa (Bend stress + Remaining Stress =Total initial stress = ~800MPa + (- 120MPa) = 680 MPa).

Zapp et al used finite-element analysis to estimate the stress in a non-welded 304L teardrop (no weld in apex).[11] The analysis was based on simulating the bending of a 10 cm long 304L strip around a 25 mm diameter mandrel. Figure 43a shows the results of that analysis superimposed on a photograph of a teardrop. Figure 43b shows a 304L teardrop after exposure to boiling magnesium chloride solution.[2] Cracking was near the weld but outside of the heat affected zone.

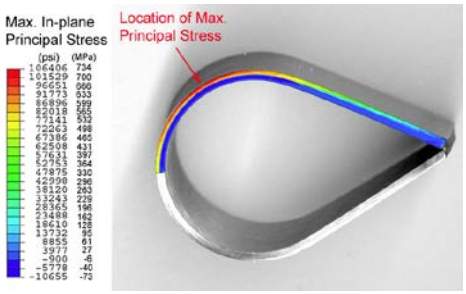

Figure 43(a). Location of stresses in a teardrop calculated using finite-element analysis**. 43(b).** 304L teardrops after exposure to boiling magnesium chloride solution.

The maximum stress calculated using finite element analysis in the teardrop, 730 MPa, was not at the apex (Figure 43a). Calculated stress in the apex was 480 MPa. The stress in the apex region determined from slitting measurements (680 MPa) is higher than the value determined by finite element analysis (480 MPa) however the finite element analysis did not include residual stresses due to welding.

Teardrops are used as screening tools in corrosion studies to evaluate factors affecting corrosion in 3013 containers and in particular the inner wall of the ICCWR in SRS/Hanford inner containers. Residual hoop stresses of 680 MPa were calculated to be present on the outer surface of a teardrop in the apex region based on slitting data. These are comparable to the residual stresses measured by incremental hole drilling on the inner

wall of an SRS/Hanford 3013 in the ICCWR (710 MPa uncorrected). The time to cracking for the 304L teardrop in the $MgCl_2$ experiments was approximately 1.3 hours compared with 2 hours for the SRS/Hanford inner container ICCWR.[2] These results support the continued use of teardrop samples as surrogates for some aspects of 3013 inner container SCC behavior studies. It is also important to be cognizant of the differences and be duly cautious in interpreting results. Higher hoop stresses (1100 MPa) were measured on the interior surfaces of the SRS/Hanford inner container using incremental hole drilling than are present in teardrops (730 MPa). Other factors such as the presence of weld oxide in the ICCWR (Zapp et. al[11]) also affect the susceptibility of 304L SS to SCC and should be incorporated in teardrop studies.

V. Conclusions

Results of residual stress measurements and calculations in various 3013 containers and teardrop samples are summarized in Table 6.

Table 6. Summary of measured and calculated residual stresses.

Container Section/Sample	Hoop Maximum Residual Stress (MPa)	Axial Maximum Residual Stress (MPa)	Location	Technique
3013 Outer	360	200	OCCWR	Neutron Scattering
	260			Contour
SRS/Hanford 3013 Inner	480		ICCWR	Contour
	800-1100	200-400		Incremental Hole Drilling
	710 (inner wall) (no release correction)	160 (inner wall) (no release correction)		
RFETS/LLNL 3013 Inner	180		ICCWR	Contour
304L Teardrop with weld	680		Apex	Split and Slit
304 L teardrop – No weld	730		Side	Finite Element Analysis
	480		Apex	

Results indicate sufficient residual stress in 3013 outer, inner and teardrop samples to result in SCC.[4] In particular, very high (yield magnitude) residual stresses were measured in SRS/Hanford inner containers and teardrop samples. Contour measurements of the 3013 inner containers indicated that the ICCWR contained the largest stresses in the measured sections. Maximum residual stresses in the SRS/Hanford inner container were more than double the maximum residual stresses observed in the RFETS/LLNL inner container. Hoop stresses were larger than axial stresses in the highest stress regions of the outer and inner containers that were measured.

VI. ACKNOWLEDGEMENTS

The authors would like to acknowledge Hunter Swenson for work on contour measurements for RFETS/LLNL container, Ted Venetz for providing the SRS/Hanford inner containers, John Mickalonis, Scott Breshears, Josh Narlesky and Mary Ann Hill, and Donald W. Brown for helpful discussions and Thomas A. Sisneros for work on the neutron diffraction measurements.. Funding for this work was provided by the Surveillance and Monitoring Program, US Department of Energy Office of Environmental Management. This work has benefited from the use of SMARTS at the Lujan Center at Los Alamos Neutron Science Center. This work was conducted at Los Alamos National Laboratory operated by Los Alamos National Security, LLC under contract DE-AC52-06NA25396 for US Department of Energy under contract DE-AC09-08SR22470.

VII. REFERENCES

1. Kolman, D. G. Review of the potential environmentally assisted failure mechanisms of austenitic stainless steel storage containers housing stabilized radioactive compounds. *Corrosion Science* 2001, *43* (1), pp 99-125.
2. Mickalonis, J., and Dunn, K.A. Residual Stresses in 3013 Containers. *Journal of Nuclear Materials Management* 2010, *38*, pp 31-38.
3. Dunn, K. A.; Louthan, M. R., Jr. Rawls, G. B.; Sindelar, R. L.; Zapp, P. E.; McClard, J. W. Container materials, fabrication, and robustness. *JNMM* 2010, *38* (2), pp 17-24.
4. Parrott, R., Pitts, H., Hill H. Derbyshire, B. *Chloride stress corrosion cracking in austenitic stainless steel*; Health and Safety Laoratory: 2011.
5. Howard, S., Daugherty, W., and Sessions, C. *Implementation of an Outer Can Welding System for Savannah River Site Plutonium Processing Facility*; Wedstinghouse Savannah River company: Aiken, South Carolina, 2003.
6. Schajer, G. S. *Practical Residual Stress Measurement Methods*. John Wiley & Sons: Chicester, UK, 2013.
7. Bourke, M. A. M.; Dunand, D. C.; Ustundag, E. SMARTS - a spectrometer for strain measurement in engineering materials. *Applied Physics A-Materials* 2002, *74*, S1707-S1709.
8. Prime, M. B., and DeWald, A. T The Contour Method In *Practical Residual Stress Measurement Methods*, G. S. Schajer, e., Ed. John Wiley & Sons, Ltd.: John Wiley & Sons, Ltd, 2013.
9. Prime, M. B., and Kastengren, A. L. The Contour Method Cutting Assumption: Error Minimization and Correction In *Experimental and Applied Mechanics*, T. Proulx, e., Ed. Springer New York, 2011; Vol. Volume 6, pp 233-250.
10. Berg, J. M., Duque, J. Joyce, S. , Kelly, E., Narlesky, J. Rios, D. Stroud, M.A., Veirs, D. K., Duffy, J., Dunn, K. , Mickalonis, J, and Scogin, J. *Technical Summary of Results of 301 Field Surveillance and Shelf-life Studies*; Los Alamos National Laboratory: 2015.
11. Zapp, P. E.; Duffey, J. M.; Lam, P. S.; Dunn, K. A.; Veirs, D. K.; Worl, L. A.; Berg, J. M. Relative humidity and the susceptibility of austenitic stainless steel to stress-corrosion cracking in an impure plutonium oxide environment. *Journal of Nuclear Materials Management* 2010, *38* (3), pp 4-14.

Table A1. Radial and hoop residual stresses measured by incremental hole drilling for location HD1 and HD2 in the H5107 container lid. Maximum tensile stresses in each column are highlighted.

Metric	H5107_HD1			H5107_HD2		
Depth (mm)	Radial (MPa)	Hoop (MPa)	Uncertainty (MPa)	Radial (MPa)	Hoop (MPa)	Uncertainty (MPa)
0.013	-261.3	374.4	30.3	-90.3	183.4	26.9
0.064	-47.6	430.2	29.0	-100.7	484.7	22.1
0.127	-26.9	310.3	29.0	-15.9	437.1	24.1
0.178	-43.4	197.9	28.3	2.1	269.6	22.8
0.229	-19.3	173.8	28.3	-6.2	206.9	22.8
0.279	2.8	173.8	28.3	-0.7	188.2	23.4
0.330	10.3	173.1	29.0	15.2	180.6	23.4
0.381	0.0	154.4	29.6	37.9	217.2	24.1
0.432	4.8	159.3	31.0	33.8	208.9	24.8
0.483	-4.1	155.8	31.7	-1.4	212.4	25.5
0.533	-15.9	150.3	33.1	-9.0	237.2	26.9
0.584	-11.7	155.1	34.5	46.9	266.1	27.6
0.635	2.8	173.8	35.9	75.8	311.7	29.0
0.686	51.0	231.7	37.9	45.5	285.5	30.3
0.737	77.2	273.0	39.3	-22.8	211.0	32.4
0.787	24.1	239.3	43.4	-57.9	181.3	36.5
0.838	-49.0	182.7	49.0	-24.1	250.3	40.0
0.889	-81.4	166.2	50.3	44.1	379.2	42.7
0.940	-86.9	173.8	81.4	137.9	453.7	76.5
0.991	-84.1	193.1	162.0	230.3	490.9	140.0

Table A2. Axial and hoop residual stresses measured by incremental hole drilling for location HD3 in the H5107 container wall at 12.5 mm below the weld toe from the inner wall outward. Results include corrections for the stresses released when the lid was cut in half at Plane 1. Maximum tensile stresses in each column are highlighted.

Metric	HD3 Measured			HD3 Released		HD3 Total	
Depth (mm)	Axial (MPa)	Hoop (MPa)	Uncertainty (MPa)	Axial (MPa)	Hoop (MPa)	Axial (MPa)	Hoop (MPa)
0.013	-491.6	-680.5	44.1	-25.7	19.4	-517.3	-661.1
0.064	-291.0	-475.8	34.5	-23.8	19.2	-314.8	-456.5
0.127	-342.0	-522.6	29.0	-21.9	19.0	-363.9	-503.6
0.178	-408.9	-579.9	25.5	-20.1	18.8	-428.9	-561.0
0.229	-433.7	-587.5	25.5	-18.2	18.7	-451.9	-568.8
0.279	-398.5	-528.8	25.5	-16.3	18.5	-414.9	-510.4
0.330	-393.0	-499.2	26.2	-14.5	18.3	-407.5	-480.9
0.381	-428.2	-512.3	26.9	-12.6	18.1	-440.8	-494.2
0.432	-437.1	-500.6	27.6	-10.7	17.9	-447.9	-482.7
0.483	-409.6	-452.3	28.3	-8.9	17.7	-418.4	-434.6
0.533	-340.6	-364.1	29.6	-7.0	17.5	-347.6	-346.5
0.584	-284.8	-290.3	30.3	-5.2	17.3	-289.9	-272.9
0.635	-251.7	-244.8	31.7	-3.3	17.1	-255.0	-227.6
0.686	-195.1	-184.1	33.8	-1.4	17.0	-196.6	-167.1
0.737	-127.6	-121.4	35.9	0.4	16.8	-127.1	-104.6
0.787	-40.0	-46.2	40.0	2.3	16.6	-37.7	-29.6
0.838	76.5	51.0	44.1	4.2	16.4	80.7	67.4
0.889	224.8	174.4	46.2	6.0	16.2	230.8	190.6
0.940	385.4	307.5	80.7	7.9	16.0	393.3	323.5
0.991	547.5	440.6	150.3	9.7	15.8	557.2	456.4

Table A3. Axial and hoop residual stresses for location HD4 in the H5107 container wall at 2.5 mm below the weld toe from the outer wall inward. Results include calculated stresses from measurements on the halved lid, released stresses when the lid was cut in half and total stresses (calculated + released). Maximum tensile stresses in each column are highlighted.

Metric	HD4 Calculated			HD4 Released		HD4 Total	
Depth (mm)	Axial (MPa)	Hoop (MPa)	Uncertainty (MPa)	Axial (MPa)	Hoop (MPa)	Axial (MPa)	Hoop (MPa)
0.013	-319.2	24.1	20.7	99.8	91.9	-219.4	116.0
0.064	-228.9	224.8	10.3	97.3	92.6	-131.6	317.4
0.127	-174.8	376.8	15.9	94.8	93.3	-80.0	470.2
0.178	-180.0	455.8	15.2	92.3	94.1	-87.7	549.8
0.229	-201.7	508.5	14.5	89.8	94.8	-111.9	603.3
0.279	-206.2	575.7	14.5	87.3	95.6	-118.9	671.3
0.330	-192.0	646.4	14.5	84.8	96.3	-107.2	742.7
0.381	-167.5	683.3	15.2	82.3	97.1	-85.2	780.4
0.432	-126.2	675.0	15.2	79.8	97.8	-46.4	772.8
0.483	-80.3	614.7	15.9	77.3	98.6	-3.0	713.2
0.533	-32.8	532.6	16.5	74.8	99.3	42.1	631.9
0.584	17.9	478.5	17.2	72.3	100.0	90.3	578.6
0.635	68.6	476.8	17.9	69.8	100.8	138.4	577.6
0.686	94.5	504.0	19.3	67.3	101.5	161.8	605.6
0.737	81.4	517.1	22.1	64.8	102.3	146.2	619.4
0.787	31.4	500.2	23.4	62.3	103.0	93.7	603.3
0.838	-48.6	446.5	24.1	59.8	103.8	11.2	550.2
0.889	-153.1	365.4	34.5	57.3	104.5	-95.7	470.0
0.940	-268.2	272.4	60.0	54.8	105.3	-213.4	377.6
0.991	-387.8	176.2	93.8	52.4	106.0	-335.5	282.2

Table A4. Axial and hoop residual stresses for location HD5 in the H5107 container wall at 12.5 mm below the weld toe from the outer wall inward. Results include calculated stresses from measurements on the halved lid, released stresses when the lid was cut in half and total stresses (calculated + released). Maximum tensile stresses in each column are highlighted.

Metric	HD5 Measured			HD5 Released		HD5 Total	
Depth (mm)	Axial (MPa)	Hoop (MPa)	Uncertainty (MPa)	Axial (MPa)	Hoop (MPa)	Axial (MPa)	Hoop (MPa)
0.013	204.8	255.8	33.1	-33.3	13.7	171.4	269.5
0.064	457.1	446.1	8.3	-31.7	13.6	425.5	459.7
0.127	669.5	599.2	19.3	-30.0	13.6	639.5	612.8
0.178	808.8	683.3	20.7	-28.3	13.6	780.5	696.9
0.229	866.0	690.2	13.1	-26.6	13.6	839.4	703.8
0.279	848.8	629.5	13.1	-24.9	13.5	823.9	643.1
0.330	783.3	534.4	16.5	-23.2	13.5	760.1	547.9
0.381	677.8	428.9	14.5	-21.5	13.5	656.3	442.4
0.432	541.9	324.8	13.1	-19.8	13.5	522.1	338.2
0.483	380.6	222.0	13.8	-18.1	13.5	362.5	235.5
0.533	204.8	111.0	13.8	-16.4	13.4	188.4	124.4
0.584	29.0	-8.3	15.2	-14.7	13.4	14.2	5.1
0.635	-134.5	-128.2	16.5	-13.0	13.4	147.5	-114.9
0.686	-275.8	-238.6	17.9	-11.3	13.4	287.1	-225.2
0.737	-392.3	-335.1	18.6	-9.6	13.3	402.0	-321.8
0.787	-486.1	-416.5	19.3	-7.9	13.3	494.0	-403.1
0.838	-560.6	-486.8	26.2	-6.2	13.3	566.8	-473.5
0.889	-618.5	-548.8	39.3	-4.6	13.3	623.0	-535.6
0.940	-668.8	-607.4	58.6	-2.9	13.2	671.7	-594.2
0.991	-716.4	-664.7	80.0	-1.2	13.2	717.6	-651.5

Table A5. Axial and hoop residual stresses HD4 in the H5107 container wall at 5 mm below the weld toe from the outer wall inward. Results include calculated stresses from measurements on the halved lid, released stresses when the lid was cut in half and total stresses (calculated + released). Maximum tensile stresses in each column are highlighted.

Metric	HD6 Measured			HD6 Released		HD6 Total	
Depth (mm)	Axial (MPa)	Hoop (MPa)	Uncertainty (MPa)	Axial (MPa)	Hoop (MPa)	Axial (MPa)	Hoop (MPa)
0.013	-251.7	36.5	24.8	47.1	86.9	204.6	123.4
0.064	-260.3	56.9	17.2	44.3	86.1	216.0	143.0
0.127	-243.0	96.2	20.7	41.4	85.3	201.6	181.5
0.178	-181.7	170.0	19.3	38.6	84.5	143.1	254.5
0.229	-123.1	231.3	19.3	35.8	83.7	-87.3	315.0
0.279	-62.1	293.7	19.3	33.0	82.9	-29.1	376.6
0.330	3.1	368.5	20.0	30.2	82.1	33.3	450.7
0.381	56.5	434.4	20.0	27.4	81.3	83.9	515.7
0.432	81.4	473.0	20.7	24.5	80.5	105.9	553.5
0.483	67.6	473.0	21.4	21.7	79.7	89.3	552.7
0.533	38.6	455.1	22.1	18.9	79.0	57.5	534.0
0.584	23.4	442.7	23.4	16.1	78.2	39.5	520.8
0.635	-6.6	401.6	24.8	13.3	77.4	6.7	479.0
0.686	-69.0	310.3	25.5	10.5	76.6	-58.5	386.9
0.737	-121.7	217.5	28.3	7.6	75.8	114.1	293.3
0.787	-115.8	182.0	31.7	4.8	75.0	111.0	257.0
0.838	-57.2	211.7	33.1	2.0	74.2	-55.2	285.9
0.889	21.4	272.4	38.6	-0.8	73.4	20.6	345.8
0.940	92.7	336.8	71.0	-3.6	72.6	89.1	409.5
0.991	154.8	393.4	122.0	-6.5	71.8	148.3	465.2

Table A6. Axial and hoop residual stresses for location HD7 in the H5107 container wall at 9 mm below the weld toe from the outer wall inward. Results include calculated stresses from measurements on the halved lid, released stresses when the lid was cut in half and total stresses (calculated + released). Maximum tensile stresses in each column are highlighted.

Metric	HD7 Measured			HD7 Released		HD7 Total	
Depth (mm)	Axial (MPa)	Hoop (MPa)	Uncertainty (MPa)	Axial (MPa)	Hoop (MPa)	Axial (MPa)	Hoop (MPa)
0.013	-143.4	67.6	27.6	-19.1	48.5	162.5	116.1
0.064	90.3	247.5	9.0	-18.0	48.3	72.3	295.8
0.127	260.6	379.9	17.2	-16.9	48.1	243.8	428.1
0.178	338.5	435.1	15.2	-15.7	48.0	322.8	483.1
0.229	342.7	425.4	13.8	-14.6	47.8	328.1	473.2
0.279	304.8	376.5	13.8	-13.5	47.7	291.3	424.1
0.330	251.7	308.9	14.5	-12.4	47.5	239.3	356.4
0.381	192.4	233.7	14.5	-11.2	47.3	181.1	281.1
0.432	111.0	164.8	15.2	-10.1	47.2	100.9	211.9
0.483	-23.4	94.5	20.0	-9.0	47.0	-32.4	141.5
0.533	-161.3	26.2	17.9	-7.8	46.8	169.2	73.0
0.584	-261.3	-36.5	16.5	-6.7	46.7	268.0	10.1
0.635	-321.3	-94.5	17.2	-5.6	46.5	326.9	-48.0
0.686	-364.7	-152.4	19.3	-4.5	46.3	369.2	-106.1
0.737	-407.5	-211.7	20.7	-3.3	46.2	410.8	-165.5
0.787	-448.9	-265.5	22.1	-2.2	46.0	451.1	-219.5
0.838	-480.6	-311.0	24.1	-1.1	45.8	481.7	-265.1
0.889	-495.8	-342.0	35.2	0.1	45.7	495.7	-296.3
0.940	-493.7	-365.4	57.9	1.2	45.5	492.5	-319.9
0.991	-482.0	-385.4	87.6	2.3	45.3	479.6	-340.1

Table A7. Axial and hoop residual stresses for location HD8 in the H5107 container wall at 2.5 mm below the weld toe from the outer wall inward. Results include calculated stresses from measurements on the halved lid, released stresses when the lid was cut in half and total stresses (calculated + released). Maximum tensile stresses in each column are highlighted.

Metric	HD8 Measured			HD8 Released		HD8 Total	
Depth (mm)	Axial (MPa)	Hoop (MPa)	Uncertainty (MPa)	Axial (MPa)	Hoop (MPa)	Axial (MPa)	Hoop (MPa)
0.013	-241.0	-10.7	22.1	124.0	222.2	-117.0	211.5
0.064	-209.3	106.5	11.0	125.0	222.3	-84.2	328.9
0.127	-186.5	203.7	16.5	126.1	222.5	-60.4	426.2
0.178	-170.3	273.7	15.9	127.2	222.6	-43.1	496.4
0.229	-140.0	338.5	15.2	128.3	222.8	-11.7	561.3
0.279	-94.5	400.6	15.2	129.3	223.0	34.9	623.6
0.330	-50.3	453.0	15.9	130.4	223.1	80.1	676.1
0.381	-21.4	490.2	15.9	131.5	223.3	110.1	713.5
0.432	-18.3	503.0	16.5	132.6	223.4	114.3	726.4
0.483	-37.6	496.1	17.2	133.7	223.6	96.1	719.7
0.533	-56.5	492.3	17.9	134.7	223.8	78.2	716.1
0.584	-51.4	514.0	18.6	135.8	223.9	84.5	737.9
0.635	-19.3	553.0	19.3	136.9	224.1	117.6	777.1
0.686	21.0	579.5	20.7	138.0	224.2	159.0	803.8
0.737	41.0	577.5	23.4	139.1	224.4	180.1	801.8
0.787	17.6	534.7	24.8	140.1	224.5	157.7	759.3
0.838	-52.4	453.7	25.5	141.2	224.7	88.8	678.4
0.889	-158.9	347.2	35.9	142.3	224.9	-16.6	572.0
0.940	-284.4	231.3	62.7	143.4	225.0	-141.1	456.3
0.991	-415.4	115.5	97.9	144.4	225.2	-271.0	340.7

Table A8. Axial and hoop residual stresses measured by incremental hole drilling for location HD9 and 10 in the H5117 container wall at 2.5 mm and 1mm below the weld toe from the outer wall inward. Maximum tensile stresses in each column are highlighted.

Metric	H5117 HD9 (Outer wall inward) 2.5 mm below weld toe			H5117 HD10 (Outer wall inward) 1 mm below weld toe		
Depth (mm)	Axial (MPa)	Hoop (MPa)	Uncertainty (MPa)	Axial (MPa)	Hoop (MPa)	Uncertainty (MPa)
0.013	-140.3	10.0	23.4	-250.3	-62.7	10.3
0.064	-111.4	81.7	14.5	-244.4	-41.7	4.1
0.127	-148.2	124.8	19.3	-239.3	-20.0	6.9
0.178	-197.9	167.5	17.9	-233.1	1.4	6.9
0.229	-218.9	204.4	17.9	-227.9	23.1	6.2
0.279	-191.7	245.5	17.9	-221.3	44.8	6.2
0.330	-167.9	295.5	17.9	-215.5	65.8	6.2
0.381	-156.2	347.2	18.6	-209.6	86.9	6.2
0.432	-155.5	411.3	19.3	-202.7	107.6	6.9
0.483	-158.6	459.2	20.0	-195.1	127.6	6.9
0.533	-159.6	481.6	20.7	-187.2	146.5	6.9
0.584	-154.4	484.0	21.4	-178.9	165.8	6.9
0.635	-158.9	476.8	22.8	-169.6	183.4	7.6
0.686	-188.2	488.9	23.4	-160.0	201.3	7.6
0.737	-236.5	542.6	26.2	-150.0	218.2	8.3
0.787	-265.8	608.5	29.6	-140.0	235.1	9.0
0.838	-253.4	643.0	30.3	-128.9	251.7	9.0
0.889	-218.9	643.0	37.9	-118.6	268.9	10.3
0.940	-186.2	639.9	69.0	-107.9	285.1	17.2
0.991	-160.3	643.6	113.8	-96.9	301.7	28.3

Table A9. Axial and hoop residual stresses measured by incremental hole drilling for location HD11 and 112 in the H5117 container wall at 2.5 mm below the weld toe from the inner wall outward. Measured results have not been corrected for partial removal of the lid.

Metric	H5117 HD11 (Inner wall outward) 2.5 mm below weld toe			H5117 HD12 (Inner wall outward) 2.5 mm below weld toe		
Depth (mm)	Axial (MPa)	Hoop (MPa)	Uncertainty (MPa)	Axial (MPa)	Hoop (MPa)	Uncertainty (MPa)
0.013	162.7	670.2	17.2	163.4	713.6	17.2
0.064	225.8	736.0	8.3	210.6	802.2	7.6
0.127	271.3	785.7	13.1	266.1	907.4	12.4
0.178	295.8	814.3	13.1	330.3	1026.7	12.4
0.229	306.8	828.1	11.7	382.7	1114.9	11.7
0.279	304.4	828.4	12.4	397.5	1135.3	11.7
0.330	299.6	827.7	12.4	379.6	1110.4	11.7
0.381	302.3	834.6	12.4	349.6	1074.9	12.4
0.432	297.9	835.7	13.1	319.6	1042.2	12.4
0.483	269.6	815.7	13.8	288.6	1009.8	13.1
0.533	217.9	772.2	14.5	254.4	972.9	13.8
0.584	169.6	735.0	15.2	213.7	921.2	14.5
0.635	135.1	712.9	15.9	162.0	857.0	15.2
0.686	108.9	700.5	17.2	99.3	791.5	16.5
0.737	83.8	689.2	19.3	28.6	736.0	18.6
0.787	44.8	666.7	20.0	-46.2	687.4	19.3
0.838	-18.3	618.8	21.4	-123.8	644.3	21.4
0.889	-110.3	543.3	32.4	-203.1	598.1	32.4
0.940	-218.9	451.3	55.2	-283.4	545.4	53.8
0.991	-334.8	352.0	83.4	-365.8	490.6	80.0

Attachment 2. Hoop stresses as a function of distance down the wall in H5107 container

Contour mid wall hoop residual stresses as a function of distance down the wall in H5107 container wall. Maximum tensile stresses in each column are highlighted.

P1 Left Wall		P1 Right Wall (weld stop)	
Distance (mm)	stress (MPa)	Distance (mm)	stress (MPa)
0.00	156.4	0.00	34.9
0.50	184.2	0.50	43.4
1.00	215.6	1.00	37.0
1.50	246.3	1.50	16.9
2.00	276.3	2.00	14.6
2.50	314.0	2.50	52.6
3.00	351.0	3.00	144.7
3.50	379.4	3.50	246.6
4.00	389.7	4.00	332.7
4.50	384.0	4.50	385.0
5.00	367.4	5.00	416.2
5.50	358.8	5.50	434.6
6.00	354.9	6.00	433.3
6.50	353.0	6.50	405.6
7.00	351.1	7.00	368.6
7.50	347.5	7.50	330.8
8.00	335.3	8.00	284.7
8.50	312.8	8.50	253.6
9.00	282.5	9.00	218.1
9.50	250.6	9.50	186.5
10.00	215.0	10.00	149.8
10.50	180.9	10.50	119.9
11.00	152.8	11.00	92.2
11.50	122.0	11.50	63.8
12.00	99.1	12.00	36.1
12.50	75.5	12.50	12.2
13.00	53.1	13.00	-9.2
13.50	35.4	13.50	-28.0
14.00	19.2	14.00	-43.3
14.50	6.5	14.50	-56.2
15.00	-4.0	15.00	-66.6
15.50	-12.2	15.50	-74.4
16.00	-19.2	16.00	-80.2
16.50	-25.6	16.50	-84.3
17.00	-31.2	17.00	-87.6
17.50	-36.2	17.50	-90.8
18.00	-40.8	18.00	-93.2
18.50	-45.4	18.50	-95.8

P2 Wall		P3 Wall	
Distance (mm)	stress (MPa)	Distance (mm)	stress (MPa)
0.00	-50.8	0.00	-26.5
0.50	11.7	0.50	7.9
1.00	80.7	1.00	35.7
1.50	148.6	1.50	54.4
2.00	218.5	2.00	72.6
2.50	280.4	2.50	98.0
3.00	338.3	3.00	142.7
3.50	396.2	3.50	209.9
4.00	445.1	4.00	265.3
4.50	472.0	4.50	303.0
5.00	482.3	5.00	322.1
5.50	483.7	5.50	326.9
6.00	476.3	6.00	320.8
6.50	461.5	6.50	304.5
7.00	435.0	7.00	277.9
7.50	410.7	7.50	250.2
8.00	384.8	8.00	223.5
8.50	356.8	8.50	200.6
9.00	328.9	9.00	181.8
9.50	301.6	9.50	165.1
10.00	279.9	10.00	150.5
10.50	256.0	10.50	135.4
11.00	233.0	11.00	121.2
11.50	206.5	11.50	107.3
12.00	184.7	12.00	96.0
12.50	160.8	12.50	85.0
13.00	137.4	13.00	75.0
13.50	115.4	13.50	66.0
14.00	96.2	14.00	56.8
14.50	80.5	14.50	48.6
15.00	65.1	15.00	39.8
15.50	51.2	15.50	31.3
16.00	38.7	16.00	22.6
16.50	29.2	16.50	15.1
17.00	19.6	17.00	6.5
17.50	10.0	17.50	-1.2
18.00	0.8	18.00	-8.1
18.50	-8.0	18.50	-14.8

Attachment 2. Hoop stresses as a function of distance down the wall in H5107 container

P1 Left Wall		P1 Right Wall (Weld stop)	
Distance (mm)	stress (MPa)	Distance (mm)	stress (MPa)
19.00	-49.6	19.00	-97.9
19.50	-53.9	19.50	-99.2
20.00	-58.4	20.00	-99.4
20.50	-63.0	20.50	-99.9
21.00	-68.0	21.00	-100.0
21.50	-73.1	21.50	-98.9
22.00	-78.6	22.00	-97.0
22.50	-84.2	22.50	-94.2
23.00	-89.4	23.00	-91.3
23.50	-94.4	23.42	-87.9
23.71	-96.2	23.92	-83.1
24.21	-100.1	24.42	-78.3
24.71	-103.7	24.92	-72.7
25.21	-106.7	25.42	-67.5
25.71	-109.1	25.92	-61.8
26.21	-111.3	26.42	-55.7
26.71	-113.3	26.92	-50.4
27.21	-115.2	27.42	-44.6
27.71	-116.9	27.92	-39.3
28.21	-118.6	28.42	-34.4
28.71	-120.1	28.92	-29.1
29.21	-121.8	29.42	-23.1
29.71	-123.7	29.92	-19.0
30.21	-125.4	30.42	-14.6
30.71	-126.9	30.92	-10.6
31.21	-127.2	31.42	-7.2
31.71	-125.5	31.92	-4.5
32.21	-122.4	32.42	-2.9
32.71	-117.4	32.92	-1.8
33.21	-110.4	33.42	-1.5
33.71	-101.5	33.92	-0.3
34.21	-90.4	34.42	1.9
34.71	-78.4	34.92	6.1
35.21	-66.2	35.42	12.1
35.71	-51.7	35.92	19.3
36.21	-35.8	36.42	27.3
36.71	-20.2	36.92	34.9
37.21	-5.0	37.42	43.8
37.71	12.7	37.92	51.7

P2 Wall		P3 Wall	
Distance (mm)	stress (MPa)	Distance (mm)	stress (MPa)
19.00	-16.3	19.00	-21.4
19.50	-23.2	19.50	-27.2
20.00	-29.3	20.00	-32.5
20.50	-34.8	20.50	-37.4
21.00	-39.0	21.00	-42.4
21.50	-42.3	21.50	-46.9
22.00	-45.1	22.00	-50.4
22.50	-47.1	22.50	-52.5
23.00	-48.8	23.00	-53.7
23.42	-50.0	23.42	-54.6
23.92	-51.7	23.92	-55.0
24.42	-52.0	24.42	-54.3
24.92	-51.8	24.92	-53.8
25.42	-51.2	25.42	-52.6
25.92	-48.9	25.92	-50.9
26.42	-46.6	26.42	-48.8
26.92	-43.6	26.92	-46.7
27.42	-40.8	27.42	-44.9
27.92	-39.3	27.92	-42.8
28.42	-37.5	28.42	-39.8
28.92	-35.0	28.92	-35.6
29.42	-33.3	29.42	-31.3
29.92	-30.1	29.92	-26.9
30.42	-25.6	30.42	-22.6
30.92	-20.3	30.92	-18.0
31.42	-13.5	31.42	-12.6
31.92	-6.8	31.92	-7.8
32.42	-0.9	32.42	-2.6
32.92	6.5	32.92	2.7
33.42	14.1	33.42	7.3
33.92	21.8	33.92	12.2
34.42	27.4	34.42	16.2
34.92	31.6	34.92	22.0
35.42	35.4	35.42	26.4
35.92	41.8	35.92	32.6
36.42	48.5	36.42	39.1
36.92	53.7	36.92	44.0
37.42	59.2	37.42	50.2
37.92	63.8	37.92	55.3

Attachment 2. Hoop stresses as a function of distance down the wall in H5107 container

P1 Left Wall		P1 Right Wall (Weld stop)	
38.21	30.1	38.42	59.6
38.71	47.9	38.92	68.5
39.21	66.2	39.42	76.7
39.71	83.4	39.92	84.2
40.21	101.0	40.42	89.3
40.71	119.6	40.92	91.2
41.21	138.3	41.42	91.3
41.71	158.5		
42.21	173.7		

P2 Wall		P3 Wall	
38.42	71.0	38.42	60.3
38.92	78.9	38.92	67.1
39.42	84.5	39.42	71.8
39.92	90.9	39.92	78.1
40.42	95.8	40.42	83.6
40.92	100.2	40.92	89.5
41.42	102.3	41.42	95.2